

1 **Comparative Analysis of MODIS, MISR and AERONET Climatology**  
2 **over the Middle East and North Africa**

3 **Ashraf Farahat**

4 Department of Physics, King Fahd University of Petroleum and Minerals, Dhahran 31261,  
5 Saudi Arabia;  
6 E-Mails: farahata@kfupm.edu.sa

7 \*Author to whom correspondence should be addressed; E-Mail: [farahata@kfupm.edu.sa](mailto:farahata@kfupm.edu.sa).  
8 Tel: (321) 541-7088  
9

10 **Abstract:**

11 Comparative analysis of MISR MODIS, and AERONET AOD products is performed  
12 over seven AERONET stations located in the Middle East and North Africa for the  
13 period of 2000 – 2015. Sites are categorized into dust, biomass burning and mixed.  
14 MISR and MODIS AOD agree during high dust seasons but MODIS tends to  
15 underestimate AOD during low dust seasons. Over dust dominated sites, MODIS/Terra  
16 AOD indicate a negative trend over the time series, while MODIS/Aqua, MISR, and  
17 AERONET depict a positive trend. A deviation between MODIS/Aqua and  
18 MODIS/Terra was observed regardless of the geographic location and data sampling.  
19 The performance of MODIS is similar over the entire region with ~64 percent of AOD  
20 within the  $\Delta\tau = \pm 0.05 \pm 0.15\tau_{AERO}$  confidence range. MISR AOD retrievals fall within  
21 84 percent of the same confidence range for all sites examined here. Both MISR and  
22 MODIS capture aerosol climatology; however few cases were observed where one of  
23 the two sensors better captures the climatology over a certain location or AOD range  
24 than the other sensor. AERONET Level 2.0 Version 3, MODIS Collection 6.1, and  
25 MISR V23 data have been used in analyzing the results presented in this study

26 **Keywords:** AOD; Remote Sensing; North Africa; Middle East; Validation  
27  
28  
29  
30

31 **1. Introduction**

32 The Middle East and North Africa host the largest dust source in the world, the Sahara Desert  
33 in North Africa that may be responsible for up to 18 percent of global dust emission (Todd  
34 et al., 2007, Bou Karam et al. 2010, Schepanski et al. 2016). The vast 650,000 km<sup>2</sup> Rub' al  
35 Khali (Empty Quarter) sand desert is a major source of frequent dust outbreaks and severe  
36 dust storms that has major effect on human activity in the Arabian Peninsula (Böer, 1997,  
37 Elagib and Addin 1997, Farahat et al., 2015).

38 Air quality over the Arabian Peninsula has received significant attention during the past 15  
39 years due to *unprecedented overall economic growth, and a booming oil and gas industry,*  
40 *however, air pollution studies are still far from complete.* Frequently blowing dust storms  
41 play a significant role in pollutant transport over the Arabian Peninsula; and major  
42 environmental pollution events such as burning of Kuwait oil fields during the 1991, Gulf  
43 War resulted in a large environmental impact on the Arabian Gulf Area (Sadiq and McCain,  
44 1993, and Farahat 2016).

45 Aerosol optical depth, AOD, (also called aerosol optical thickness, AOT) as a parameter  
46 indicates the extinction of a beam of radiation as it passes through a layer of atmosphere that  
47 contains aerosols. Both satellites and ground-based instruments can be used to measure AOD  
48 in the atmosphere, but within the same temporal coordinates and geographic location  
49 different instruments could generate different retrievals (Kahn et al., 2007, Kokhanovsky et  
50 al., 2007, Liu et al., 2008 and Mishchenko et al., 2009).

51 Since the turn of the 21<sup>st</sup> century, an upward trend of remotely sensed and ground-based  
52 AOD and air pollutants was observed over the Middle East and North Africa (El-Askary  
53 2009, Ansmann et al. 2011, Yu et al. 2013, Chin et al. 2014, Yu et al. 2015, Farahat et al.  
54 2016, Solomos et al. 2017). This positive trend is attributed to the increase in the Middle  
55 Eastern dust activity (Hsu et al., 2012) due to changes in wind speed and soil moisture  
56 (Ginoux et al. 2001 and Kim et al. 2013). Yu et al., (2015) concluded that the persistent La

57 Niña conditions (Hoell et al., 2013) have caused increment in Saudi Arabian dust activity  
58 during 2008 – 2012. Energy subsidies also encourages energy overconsumption in the  
59 Middle East and North Africa with little incentive to adopt cleaner technology. Lack of  
60 applying strict environmental regulations have permitted exacerbated urban air pollution.  
61 During the last two decades, a large number of satellites, ground stations and computational  
62 models contributed to build global and regional maps for the temporal and spatial aerosol  
63 distributions. While, ground-based stations and field measurements can identify aerosols  
64 properties over specific geographic locations, the sparse and non-continues data from ground-  
65 based sensors scattered over the Middle East and North Africa is not sufficient to provide  
66 information on spatial and temporal trends of particulate pollution. On the other hand,  
67 satellites imagery could provide a significant source of data mapping over larger areas.  
68 For its wide spatial and temporal data availability space-born sensors are important sources  
69 to understand aerosols characteristics and transport, however low sensitivity to particle type  
70 under some physical conditions, high surface reflectivity, persistent cloud, and generally low  
71 aerosol optical depth could limit satellite data application in characterizing properties of  
72 airborne particles, especially in the Middle East.

73 In order to evaluate the efficiency of space-borne sensors in representing ground observations  
74 recorded by AERONET stations we have performed detailed statistical inter-comparison analysis  
75 between satellite AOD products and AERONET for seven stations in the Middle East and North  
76 Africa representative for dust, biomass burning, and mixed aerosol conditions (Dubovik et al.,  
77 (2000, 2002, 2006), Holben et al. (2001), Derimian et al., (2006), Basart et al. (2009), Eck  
78 el. (2010), Marey et al., 2010, Abdi et al., (2012)). Previously we analysed these seven  
79 AERONET stations to understand particles categorization and absorption properties (Farahat  
80 et al. 2016), and the current study extends the analysis to the satellite datasets.

81 In the first part of this article, we validated MISR and MODIS retrievals against collocated  
82 AERONET observations. We also assessed the consistency in aerosol trends between space-  
83 borne sensors and ground-based data.

84 In the second part, we evaluated representativeness of satellite-derived aerosol climatology  
85 over the study region from the long-term AERONET data for MISR and MODIS AOD  
86 products. It is especially relevant for the MISR instrument, as its sampling is limited by once  
87 per week observations of the same region from the two overlapping paths. MODIS provides  
88 nearly daily observations to the same geographic location; however, the quality of the product  
89 diminishes over the bright targets potentially affecting MODIS-derived aerosol climatology.  
90 The collocated MISR, MODIS and AERONET data were obtained at the MAPSS website  
91 (<http://giovanni.gsfc.nasa.gov/mapss.html>).

92

## 93 **2. Materials and Methods**

### 94 **2.1 MISR**

95 The Multi-angle Imaging SpectroRadiometer (MISR) instrument to measures tropospheric  
96 aerosol characteristics through the acquisition of global multi-angle imagery on the daylight  
97 side of Earth. MISR applies nine Charge Coupled Devices (CCDs), each with 4 independent  
98 line arrays positioned at nine view angles spread out at nadir, 26.1°, 45.6°, 60.0°, and 70.5°.  
99 In each of the nine MISR cameras, images are obtained from reflected and scattered sunlight  
100 in 4 bands blue, green, red, and near-infrared with a centre wavelength value of 446, 558,  
101 672, and 867 nm respectively. The combination of viewing cameras and spectral wavelengths  
102 enables MISR to retrieve aerosols AOD over high reflection surfaces like deserts.

103 In this study, we use Level 2 (ver. 0023) AOD at 558 nm (green band) measured by MISR  
104 instrument with a 17.6 km resolution aboard the Terra satellite. MISR Level 2 aerosol  
105 retrievals use only data that pass angle-to-angle smoothness and spatial correlation tests

106 (Martonchik et al. 2002), as well as stereoscopically derived cloud masks and adaptive cloud-  
107 screening brightness thresholds (Zhao and Di Girolamo, 2004).

## 108 **2.2 MODIS**

109 The Moderate Resolution Imaging Spectroradiometer (MODIS) is a payload instrument on  
110 board the Terra and Aqua satellites. Terra's and Aqua orbit around the Earth from North to  
111 South and South to North across the equator during the morning and afternoon respectively  
112 (Kaufman et al., 1997). Terra MODIS and Aqua MODIS provides nearly daily coverage of  
113 the Earth's surface and atmosphere in 36 wavelength bands, ranging from 0.412 to 41.2  $\mu\text{m}$ ,  
114 with spatial resolutions of 250 m (bands 1-2), 500 m (bands 3-7), 1000 m (bands 8-36).  
115 Located near-polar orbit (705 km), MODIS has swath dimensions of 2330 km  $\times$  10 km and  
116 a scan rate of 20.3 rpm. With its high radiometric sensitivity and swath resolution MODIS  
117 retrievals provides information about aerosols optical and physical characteristics. MODIS  
118 uses 14 spectral band radiance values to evaluate atmospheric contamination and determine  
119 whether scenes are affected by cloud shadow (Ackerman et al., 1998).

120 The MODIS dark-target algorithm is designed aerosol retrieval from MODIS observations,  
121 over dark land surfaces (low values of surface reflectance) (e.g., dark soil and vegetated  
122 regions) in parts of the visible (VIS, 0.47 and 0.65  $\mu\text{m}$ ) and shortwave infrared (SWIR, 2.1  
123  $\mu\text{m}$ ) spectrum (Kaufman et al., 1997). Level 2 (C006) of the algorithm are used to retrieve  
124 MODIS aerosols' time series data. Levy *et al.* (2010) reported that the dark-target algorithm  
125 AOD at 550 nm measurement for (C005) includes uncertainty of  $\pm (0.05\tau+0.03)$  and  $\pm$   
126  $(0.15\tau+0.05)$  over ocean and land respectively. This uncertainty is caused by uncertainties in  
127 computing cloud masking, surface reflectance, aerosol model type (e.g., single scattering  
128 albedo), pixels selections and instrument calibration.

## 129 **2.3 AERONET**

130 The Aerosol Robotic Network (AERONET) (Holben et al., 1998 and Holben et al., 2001) is  
131 a ground-based remote sensing aerosols network that provides a long-term data related to  
132 aerosol optical, microphysical and radiative properties. With over 700 global stations, the  
133 AERONET data is widely used in validating satellite retrievals (Chu et al., 1998 and  
134 Higurashi et al., 2000).

135 The sun photometers used by AERONET measure spectral direct-beam solar radiation, as  
136 well as directional diffuse radiation in the solar almucantar. The former are used to determine  
137 columnar spectral AOD and water vapour, provided at a temporal resolution of  
138 approximately 10–15 min (Sayer et al. 2014). AERONET direct-sun AOD has a typical  
139 uncertainty of 0.01–0.02 (Holben et al., 1998) and is provided at multiple wavelengths at  
140 340, 380, 440, 500, 675, 950, and 1020 nm.

141 Seven AERONET sites were selected for satellite validation in this study (Table 1.). The sites  
142 were selected based on their geographic locations to represent aerosols characteristics over  
143 North Africa and the Middle East (Farahat et al., 2016). A record of long-term data collection  
144 was another factor in the selection process.

#### 145 **Data Matching Approach**

146 Multi-sensors data matching requires using only compatible data to eliminate uncertainties  
147 associated with cloud shadow and spatial and temporal retrievals produced by different  
148 instruments (Liu and Mishchenko (2008) and Mishchenko et al., 2009).

149 The comparison of MISR and MODIS products against AERONET is performed to evaluate  
150 satellites' retrieval over individual North Africa and Middle East sites (see Table 1). There  
151 is only a small number of AERONET measurements that are perfectly collocated with  
152 MODIS and MISR. One way to work with this lack of compatibility problem is to compare  
153 satellites measurements nearby a certain AERONET site and comparing AERONET  
154 measurements nearly synchronized with the satellite overpass time (Sioris et al. 2017).

155 Another reasonable strategy is to average all satellite measurements with a certain distance  
156 of an AERONET location and average all AERONET measurements within a certain time  
157 range (Mishchenko et al., 2010). The results presented in this paper are based on the second  
158 approach as it compares average spatial satellite measurements with average temporal  
159 AERONET measurements. We implemented the Basart et al., (2009) approach in using a  
160 spatial and temporal threshold of 50 km and 30 min for MISR, MODIS, and AERONET data  
161 matching.

162 We use the Giovanni Multi-sensor Aerosol Products Sampling System MAPSS  
163 (<http://giovanni.gsfc.nasa.gov/aerostat/>) for the data inter-comparison as aerosols products  
164 are averaged from measurements that are within a radius of ~ 27.5 km from the AERONET  
165 station and within 30 min of each satellite flyover over this location. These data are  
166 represented in the article by MISR / MODIS “matched AERONET data”.

167 “All data” represents AOD products at the selected station. AERONET station ‘all data’  
168 are obtained through AEROSOL ROBOTIC NETWORK (AERONET) website  
169 (<https://aeronet.gsfc.nasa.gov/>). Daily AOD data with level 2.0 quality was used in the  
170 analysis (Smirnov et al., 2000) . Level 2.0 AOD retrievals are accurate up to 0.02 for mid-  
171 visible wavelengths.

172 MISR ‘all data’ is available through MISR website ([https://www-  
173 misr.jpl.nasa.gov/getData/accessData/](https://www-misr.jpl.nasa.gov/getData/accessData/)).

174

### 175 **3. Statistics**

176 We have used two statistical parameters to compare data retrievals from space-borne and  
177 ground based sensors including:

178 (1) Correlation coefficient (R),

179 The correlation coefficient is a parameter to measure data dependence. If the value of R is  
180 close to zero, it indicates weak data agreement. And values close to 1 or -1 indicate that data  
181 retrievals are positively or negatively linearly related (Cheng et al., 2012).

182

183 (2) Good Fraction (G- fraction).

184 The G- fraction indicator uses a data confidence range defined by MISR and MODIS  
185 (Bruegge et al., 1998 and Remer et al., 2005) over the land and ocean that combines absolute  
186 and relative criterion and weights data equally such that small abnormalities will not affect  
187 the inter-comparison statistics (Kahn et al., 2009). In this study, we use MODIS confidence  
188 range which defines data retrieval as “good” if the difference between MODIS and  
189 AERONET is less than

$$190 \Delta\tau = \pm 0.03 \pm 0.05\tau_{AER}, \text{ Over ocean,} \quad (1)$$

$$191 \Delta\tau = \pm 0.05 \pm 0.15\tau_{AER}, \text{ Over land.} \quad (2)$$

192

193 where  $\tau_{AER}$  is the optical depth retrieved using AERONET stations. The G-fraction is the  
194 percentage of MODIS data retrievals that satisfies (Equations (1) and (2)) over ocean and  
195 land respectively. Optical depth threshold over land (Equation (1)) is higher than over ocean  
196 (Equation (2)) due to harder data retrievals and high data instability over land.

197 A good aspect of using data confidence range is excluding small fraction data outliers from  
198 producing inexplicably large influence on comparison statistics by weighting all events  
199 equally.

200

## 201 **4. Results and discussion**

### 202 **4.1 Validating MISR and MODIS AOD retrievals against AERONET observations** 203 **over the Middle East and North Africa**



204 Illustrated in Figures 2, 3 and Tables 2, 3 is a regression analysis of MISR and MODIS Terra  
205 AOD products against AERONET AOD over the seven AERONET sites, shown in Table1,  
206 from 2000 – 2015.

207 The correlation coefficient between MISR and AERONET AOD at region 1 is equal to or  
208 above 0.85 except in Bahrain during DJF and JJA (Figure (2) and Table 2), which could be  
209 attributed to lack of data and the impact of water surface reflectivity over Bahrain. Similar  
210 correlation coefficient values were found in region 2 where MISR-AERONET AOD shows  
211 less error than MODIS (Figures (2, 3) and Table 3). In general, MODIS-AERONET AOD  
212 correlation coefficient is lower than those of MISR at all sites, except Mezaira, where MISR  
213 and MODIS matched AERONET AOD correlation almost match. The lowest MODIS-  
214 AERONET AOD correlation coefficient was found over Cairo but could be attributed to the  
215 lack of data availability at this location (Figs 3e-h). Low values of MODIS-AERONET  
216 correlation coefficient is also found over Saada, Taman, and Sedee Boker sites.

217 Over all AERONET stations, the number of MODIS AERONET matched AOD are 4 to 8  
218 times those of MISR which is expected from the MISR's sampling.

219 Comparisons show that the difference between MISR and MODIS retrievals at the selected  
220 AERONET sites could be significant as expected from the MODIS Dark Target algorithm  
221 performance over bright land surfaces Kokhanovsky et al. (2007).

222 High AOD values over regions 1 and 2 measured by both AERONET and satellites' sensors  
223 indicate higher dust activities that peaks during May – Aug during dust storms season. Higher  
224 AOD values recorded during SON over Cairo station could be caused by seasonal rice straw  
225 burning by farmers in Cairo, an environmental phenomena known as Cairo Black cloud  
226 (Marey et al. 2010). As shown in (Figure (3)), the daily variability in MODIS measurements  
227 is larger than those of MISR at all the three regions. In general, MODIS tends to  
228 underestimate the AOD values on low dust seasons (Figures (2, 3) and Tables 2, 3).

229 The MODIS underestimated AOD values are more noticeable over Bahrain. This could be  
230 attributed to large water body surrounding Bahrain, which should affect surface reflectivity.  
231 Moreover, water in the Arabian Gulf has been polluted in recent years (Afnan 2013), leading  
232 to possible changes in watercolour and uncertainties in calculating surface reflectivity. The  
233 patchy land surface or pixel grid contaminated by water body is the dominant error sources  
234 for MODIS aerosol inversion over the land areas (He et al. 2010).  
235 Compared to MODIS, MISR's outperform in retrieving AOD over region 1 including vast  
236 highly reflecting desert areas can be attributed to its multispectral and multi-angular  
237 coverage, which make MISR provide better viewing over a variety of landscapes.  
238 Meanwhile, MISR retrieval also takes into consideration aerosols' particles nonsphericity,  
239 which could have significant effect on its AOD retrievals (von Hoyningen-Huen and Posse  
240 1997). MISR's retrieval did not perform well over Cairo site due to lack of matched points  
241 in most of the seasons (15 in DJF, 39 in MAM, 61 in JJA, and 23 in SON during 2000 -  
242 2015).

243

#### 244 **4.2 Trends of AOD MISR, MODIS, and AERONET retrievals over the Middle East** 245 **and North Africa**

246 Figure 4 shows time series of monthly mean AOD derived from MODIS/Aqua,  
247 MODIS/Terra, MISR and AERONET over a) dust b) biomass and c) mixed dominated  
248 aerosol regions. The satellite AOD trends are calculated from the data collocated with  
249 AERONET observations.

250 MODIS/ Aqua and MISR AOD at Solar Village have positive trends, while MODIS/ Terra  
251 AOD have negative trends along time series (Fig. 4a). MODIS-Aqua AOD differ from those  
252 of MODIS-Terra. Discrepancy between Aqua and Terra retrievals could be related to

253 instrument calibration, or the difference in aerosol and cloud conditions from the morning to  
254 the afternoon. Both MODIS Aqua and Terra are underestimating AOD at Solar Village.  
255 MISR AOD trend shows a better agreement with Solar Village AERONET AOD as  
256 compared to MODIS.

257 Both MODIS/Aqua and MODIS/Terra AOD show a stable trend over time at Mezaria site  
258 (not shown in the figure) with a correlation coefficient of 0.11 and 0.04 respectively.  
259 MODIS/Aqua AOD over Bahrain (not shown in the figure) show, less time trend stability  
260 compared to those at Solar Village with a correlation coefficient 0.63. MODIS/Aqua,  
261 MODIS/Terra, and MISR AOD depicts a positive trend over Cairo (Fig. 4b). Taman site  
262 (Fig. 4c): MODIS/Aqua, MODIS/ Terra, MISR AOD agrees with Taman AERONET on a  
263 positive trend indicating data stability over this site.

264 Long-range (2000 – 2015) tendency indicates that contradictory AOD trend of Terra and  
265 Aqua is site-dependent and does not necessarily apply everywhere.

266 AOD difference between Terra and Aqua could be used as another indicator of the long-  
267 range satellites performance. AOD difference (Terra AOD minus Aqua AOD) varies from -  
268 0.01 to 0.19, -0.10 to 0.18, -0.02 to 0.13 over Solar Village, Taman, and Cairo respectively  
269 (Fig. 5). Over the Solar Village, Terra overestimates AOD during 2002-2004 and  
270 underestimates the AOD after 2005. Although Cairo and Taman show similar trend however  
271 over/underestimation amount is not unique for all sites. This is an indication that Aqua and  
272 Terra retrievals disagreement takes place regardless of the region but site sampling has  
273 significant effect on the amount of contradiction.

274 Statistical comparison between MISR and MODIS/Terra AOD at corresponding AERONET  
275 stations is performed by calculating G-fraction using of  $\Delta\tau = \pm 0.05 \pm 0.15\tau_{AERO}$  as a  
276 confidence interval. Over the region 1, MISR AOD retrievals are more accurate than MODIS  
277 retrievals. MODIS, however, performs better over region 2 sites with high percentage of the

278 data points falling within the confidence range (Tables 2 and 3). High light reflections from  
279 the desert landscape surrounding region 1 could have an effect on MODIS retrievals.  
280 Excluding Bahrain and Cairo for low data retrievals the performance of MODIS tends to be  
281 similar over all region with  $\sim 64$  percent of AOD retrievals fall within the  
282  $\Delta\tau = \pm 0.05 \pm 0.15\tau_{AERO}$  confidence range of the AERONET AOD while MISR retrievals  
283 show better performance with  $\sim 84$  percent of the data falling within the same confidence  
284 range. This could be attributed to low number of retrievals available for Bahrain and Cairo  
285 compared to other sites. Vast sea region surrounding Bahrain and complex landscape in Cairo  
286 could also have an impact on retrievals.

### 287 **4.3 Evaluating the MISR and MODIS climatology over Middle East and North Africa**

288 Comparisons between MISR and MODIS AOD at selected AERONET stations over the  
289 2000 – 2015 period are illustrated in Figures 6- 12.

290 Figure (6a, b) shows histogram of the MISR, MODIS and AERONET AOD at Solar Village  
291 for MISR and MODIS data points collocated with AERONET observations. The mean,  
292 standard deviation, and number of measurements are also presented.

293 MISR tends to underestimate the frequency of low AOD compared to AERONET but  
294 overestimate the frequency of high AOD. MISR histograms show prominent peaks at 0.50  
295 that can be also observed in AERONET and at 0.75 that could not be seen in AERONET.  
296 MISR and AERONET AOD climatology agree well with one another. MODIS also tends to  
297 underestimate the frequency of low AOD events and overestimate the frequency of high  
298 AOD events. High surface reflectance could cause overestimation in MODIS AOD (Ichoku  
299 et al., 2005). Both MISR and MODIS provide a good representation of the AOD climatology  
300 as compared to AERONET at the Solar Village. Mezaria station, which is located in an arid  
301 region in the UAE, has a similar climatology to the Solar Village site with dust dominating

302 aerosol. Figure (7a, b) shows histograms of the MISR, MODIS and AERONET AOD at  
303 Mezaria.

304 Similar to the Solar Village, there is a big difference between the number of samples in the  
305 matched data set and full AERONET climatology. For MISR there are 213 matched cases  
306 and for MODIS there are 498 compared to the 2245 for the entire site. This has an impact on  
307 the overall assessment showing significant differences between the matched data and the full  
308 climatology for both MISR and MODIS. First, for the MISR case, the matched AERONET  
309 data have the highest frequency at AOD of 0.15 and 0.35, but the climatology shows the  
310 highest frequency at an AOD of 0.25. AOD in the range of 0.25 to 0.30 are undersampled  
311 relative to the climatology, and AOD more than 0.35 matches the climatology with less than  
312 2 percent AOD greater than 0.85. MODIS matched AERONET data show prominent peaks  
313 at 0.3 and 0.4 compared to the climatology that has a single peak at 0.30.

314 For AOD values between 0.25 and 0.40 MODIS data were found to be under-sampled similar  
315 to MISR data between 0.65 to 0.70 and at 0.35.

316 MISR AOD retrievals matched to AERONET capture the variability in the distribution, but  
317 as in the case of Solar Village the frequency of low AOD events is underestimated but the  
318 frequency of high AOD events matched AERONET data. MISR also capture events with  
319 AOD greater than 1. A similar situation is seen in the MODIS comparison, but MODIS  
320 appears to do a better job capturing the overall shape of the AERONET AOD histogram for  
321 this site.

322 The Bahrain AERONET site is located in Manama fairly close to the Arabian Gulf, a location  
323 very different from the previous two sites. The site is also located in an urban area suffers  
324 from significant load of anthropogenic aerosols as a consequence of rapid aluminium  
325 industrial development (Farahat 2016). Figure (8a, b) shows histogram of the MISR, MODIS  
326 and Bahrian AERONET measurements with statistical analysis displayed. The AERONET

327 data matched to MISR show significant peaks at 0.20, 0.30, 0.45, 0.55, 0.7, 0.8, and 0.95 not  
328 seen in the all data climatology that has peaks at 0.55 and 0.70. AOD less than 0.15 are not  
329 representative in the matched data set at all. MISR is representing the peaks at 0.45 in the  
330 matched data set but misses the peaks at 0.20, 0.30, and 0.35. The MISR climatology agrees  
331 well with the AERONET all data climatology for all AOD. MODIS on the other hand shows  
332 an extremely large frequency of AOD at 0.1 not represented by AERONET coupled with an  
333 underestimation of AOD greater than 0.3. This could be attributed to the size of the matching  
334 window and MODIS retrievals preferentially coming from the Arabian Gulf.

335 SAADA station is located close to some hiking trails at the Agoundis Valley in the Atlas  
336 Mountains about 197 km from the city of Marrakesh.

337 MISR AOD matched to AERONET agree well with MISR full climatology retrievals over  
338 SAADA station. Both retrievals slightly underestimate SAADA full climatology and over  
339 estimate SAADA matched data retrievals at AOD equal to 0.2 while show good agreement  
340 for AOD greater than 0.2. MODIS matched to AERONET retrievals overestimate the  
341 frequency of AOD greater than 0.3. While MODIS AOD matched to AERONET captures  
342 climatology at AOD between 0.2 to 0.25, AOD frequency retrievals are under-sampled at  
343 AOD between 0.1 to 0.15 with about 13 % less events than SAADA all data retrievals at  
344 AOD equal to 0.1.

345 Figure (9a, b) indicates right skewed distribution of SAADA AOD towards small AOD  
346 values with 10.3 % and 30.1 % of AOD > 0.4 as measured by MISR and MODIS  
347 respectively. Taking into consideration MODIS overestimation we conclude that SAADA  
348 site is characterized by small AOD values and this could be related to the land topology  
349 where the station is located.

350 While MISR is capturing high AOD climatology over SAADA, both MISR and MODIS  
351 are underestimating the frequency of lower AOD events. Nevertheless, MISR captures the  
352 climatology of AOD less than 0.1 missed by MODIS retrievals.

353 Taman AERONET station is located at the oasis city of Tamanrasset, which lies in Ahaggar  
354 National Park in southern Algeria.

355 Figure (10 a, b) depicts that Taman AERONET AOD climatology is similar to those at  
356 SAADA and has a high frequency of low AOD events. Both MISR AOD matched to  
357 AERONET and MISR all data do not well capture the frequency of AOD less than 0.1 or  
358 larger than 1 while well describe the climatology for AOD in the range of 0.1 to 1. MODIS  
359 AOD matched data to AERONET correctly describe climatology with slight overestimation  
360 of AOD frequencies between 0.05 – 0.15 while not capturing AOD frequencies greater than  
361 1. MISR and MODIS show similar prominent peaks at 0.1 and 0.25 not observed in Taman  
362 AERONET AOD climatology, with more peaks observed by MISR at 0.5, 0.75, and 0.85.

363 Average AOD in SAADA and Taman is ~ 50 percent less than observed at Solar Village,  
364 Mezaria, and Bahrain sites.

365 Except for AOD greater than 1 where ground observations could be more robust, both MISR  
366 and MODIS retrievals can provide very good climatology matching over Taman site.

367 Taking into consideration lower number of MISR matching AERONET observations  
368 compared to MODIS ~ 21 and 49 percent over SAADA and Taman respectively, MISR is  
369 outperforming over these two sites, which can be attributed to its multiangle viewing  
370 capabilities over complex terrains including mountainous areas (Atlas Mountains).

371 Cairo is a mega city well known for its high pollution due to traffic and agriculture activities.  
372 MISR and MODIS matched data correctly capture AOD climatology over Cairo compared  
373 to AERONET as shown in Figure (11a, b). MISR retrievals collocated with AERONET over  
374 estimate prominent peaks of AERONET AOD at 0.15 – 0.35 while underestimate

375 AERONET AOD greater than 0.35. MISR 'all data' AOD climatology over Cairo station  
376 agrees better with AERONET AOD climatology vs. collocated dataset with some  
377 oversampling at 0.25. Frequency of high AOD retrievals greater than 0.8 have not been  
378 captured by MISR matched or all data retrievals. MODIS matched to AERONET AOD are  
379 also able to well present Cairo climatology data with a high overestimation of AOD  
380 frequency between 0.05 - 0.2 and an underestimation of AOD larger than 0.4.

381 The complex landscape and local emissions in Cairo could impose major challenges in  
382 MODIS AOD retrievals. Moreover, Cairo is one of the most densely populated cities in the  
383 world that hosts major commercial and industrial centers in North Africa. Cairo also has  
384 complicated aerosols structure developed by long range transported dust in the spring,  
385 biomass burning in the fall, strong traffic and industrial emissions (Marey et al., 2010).

386 Over Cairo station, MODIS correctly represents ground observations for AOD between 0.2  
387 - 0.4 while MISR all data better represents AOD climatology for AOD greater than 0.4.  
388

389 MISR, MODIS climatology at SEDEE Boker are illustrated in Figures (12a, b).

390 MISR 'matched' AOD frequency show significant underestimation for AOD less than 0.2  
391 and an overestimation between 0.2 – 0.4 compared with AERONET retrievals. MISR  
392 correctly captures the climatology for AOD events greater than 0.4. MISR 'matched' and 'all  
393 data' retrievals peaks at 0.2 producing high frequency of AOD oversampling compared to  
394 AERONET. MISR data retrievals do not capture the climatology for AOD less than 0.1 over  
395 this site coincident with what was previously observed over other sites. MODIS matched  
396 AERONET data underestimates frequency of AOD less than 0.2 while overestimates the  
397 frequencies between 0.2 - 0.6, and well match frequencies of higher AOD events larger than  
398 0.6. MODIS retrievals are characterized by two prominent peaks at 0.1 and 0.25 that are not  
399 found in the AERONET matched data.



400 At Sedee, MISR and MODIS retrievals are better in matching frequency of high AOD  
401 retrievals (greater than 0.4) than the frequency of low AOD. This could be an effect of  
402 possible long-range transport to Sedee Boker site (Farahat et al. 2016) along with complex  
403 mixtures of dust, pollution, smoke, and sea salt that could result in uncertainties in MISR and  
404 MODIS aerosol model selection.

405 In the summary, MISR tends to overestimate AOD > 0.4 over Solar Village, Bahrain and  
406 underestimate AOD > 0.4 over Cairo. MISR retrievals also match AOD > 0.4 for Mezaria  
407 and Sedee Boker, while agree with AERONET over SAADA and Taman at all ranges of  
408 AOD. This could be expounded by insufficient particle absorption in MISR algorithm (Kahn  
409 et al., 2005). Spherical particle absorption is produced by externally mixing small black  
410 carbon particles.

411 Percentage of MISR, MODIS, and AERONET AOD greater than 0.4 recorded is shown in  
412 Table 4. Over Solar Village, both MISR and MODIS well capture high AOD greater than  
413 0.4 with very good agreement with the ground observations. Over Mezaria, both MISR and  
414 MODIS are over estimating the percentage of AOD greater than 0.4 by about 17.7 and 12.7  
415 percent respectively. MISR all data agrees well with AERONET all data in representing high  
416 AOD over Bahrain while MODIS shows significant under-representation of those events by  
417 about 13 percent, less than reported by Bahrain AERONET station. At SAADA, MISR AOD  
418 agrees with AERONET in showing low percentage of AOD greater than 0.4, while MODIS  
419 retrievals overestimate percentage by about 24 percent. MISR AOD over Taman AERONET  
420 station shows very good agreement, while MODIS is slightly underestimating AOD. Among  
421 all seven sites considered in this study, Sedee Boker shows lowest occurrence of AOD greater  
422 than 0.4, which is confirmed by both MISR and MODIS retrievals. Cairo AERONET records  
423 the highest frequency of AOD > 0.4, however this is largely underestimated by both MISR  
424 and MODIS retrievals.

425 It can concluded from the previous discussion that atmosphere around SAADA, Taman,  
426 and Sedee Boker sites is relatively clean and aerosol loads are small compared to Solar  
427 Village, Mezaria, Bahrain, and Cairo, however this could be affected by the location where  
428 AERONET station is installed for example SAADA and Taman stations are installed in a  
429 remote mountainous region away from urbanization while Cairo station is installed in the  
430 middle of large residential region with significant local emissions.

431

### 432 **Conclusion**

433 The performance of MODIS, MISR retrievals with corresponding AERONET  
434 measurements over different geographic locations in the Middle East and North Africa was  
435 investigated during 2000 – 2015.

436 Long-range observations show dissimilar AOD trends between MODIS/Aqua,  
437 MODIS/Terra, MISR and AERONET measurements. MODIS/Aqua matched AERONET  
438 retrievals show stable trend over all sites while, MODIS/Terra matched AERONET retrievals  
439 show significant downward trend indicating possible changes in the sensor performance.

440 MISR matched AERONET AOD data depict high correlation compared to  
441 AERONET indicating good agreement with ground observations with about 84 percent of  
442 AOD retrievals fall within the expected confidence range.

443 Consistency of MODIS and AERONET AOD vary based on the season, study area,  
444 and dominant aerosols type with about 64 percent of the retrieved AOD values fall within  
445 expected confidence range with the lowest performance over mixed particles regions.

446 Comparing satellites' AOD retrievals with corresponding AERONET measurements  
447 show that space-borne data retrievals accuracy can be affected by landscape, topology, and  
448 AOD range at which data is retrieved.

449 Few AERONET sites are verified where MISR and MODIS retrievals agree well with  
450 ground observations, while other sites only MISR or MODIS could correctly describe the  
451 climatology.

452 The AOD range at which MISR or MODIS could correctly describe ground  
453 observation is also investigated over different AERONET sites. Over Solar Village both  
454 MISR and MODIS tend to underestimate the frequency of low AOD and overestimate the  
455 frequency of high AOD compared to AERONET with MISR histograms show prominent  
456 peaks at 0.50 that matched AERONET data and 0.75 that could not be recorded in  
457 AERONET. MISR can capture the frequency of AOD greater than 1 mostly missed by  
458 MODIS. Both MISR and MODIS are found to provide good representation of the AOD  
459 climatology over the Solar Village site.

460 Similar to Solar Village, MISR underestimates frequency of lower AOD and  
461 overestimate frequencies of high AOD over Mezaria. MISR is able to correctly capture the  
462 frequency of AOD greater than 1, while MODIS retrievals are found to better represent the  
463 overall climatology. This is due to low number of MISR – matched AERONET retrievals  
464 compared to MODIS over this site. Prominent peaks at 0.3 and 0.4 were observed in MODIS  
465 matched Mezaria retrievals compared to the climatology, which has a single peak at 0.30.

466 Large water body surrounding Bahrain makes MODIS data preferentially originate  
467 from the Arabian Gulf which produces an extremely large frequency of AOD at 0.1 not  
468 observed in AERONET measurements paired with an underestimation of AOD greater than  
469 0.3. Meanwhile, MISR retrievals agree well with AOD climatology over Bahrain.

470 MISR AOD retrievals slightly underestimate SAADA climatology while show good  
471 agreement for AOD greater than 0.1. MODIS retrievals underestimate the frequency of AOD  
472 retrievals between 0.1 to 0.15, match climatology at AOD between 0.2 to 0.25, and  
473 overestimate the frequency of AOD greater than 0.3. SAADA site is characterized by small

474 frequency of low AOD values and this could be related to the landscape nature surrounding  
475 Saada station. MISR is found to be outperforming over Saada and Taman stations which can  
476 be attributed to its viewing multispectral and multiangular capabilities over mountainous  
477 regions.

478 MISR retrievals well capture prominent peaks of AERONET data at 0.15 to 0.35  
479 with small underestimation observed at AOD greater than 0.3 over Cairo. Using either MISR  
480 matched data or MISR all data over Cairo was found to do a good job in describing the  
481 climatology over this station. MODIS data retrievals are also able to well present Cairo  
482 climatology with a high overestimation of AOD frequency between 0.05 to 0.2 and an  
483 underestimation of AOD larger than 0.4. While both MISR and MODIS well describe  
484 climatology over Cairo station, MODIS can correctly represent ground observations between  
485 0.2 to 0.4.

486 Over Sedee Boker both MISR and MODIS retrievals well describe the climatology however  
487 they are more successful in matching frequency of high AOD greater than 0.4.

488 Based on analysing frequency of AOD greater than 0.4, it was found that Saada, Taman, and  
489 Sedee Boker are having better air quality compared to other sites while Cairo was found to  
490 be the most polluted site.

491 Results presented in this study are important in providing a guideline for satellites retrievals  
492 end users on which sensor could provide reliable data over certain geographic location and  
493 AOD range.

494 Adjacent geographic location and local climate among sites does not always  
495 guarantee that same sensor will provide consistent retrievals over all sites. For example, Solar  
496 Village, and Bahrain AERONET are surrounded by large desert regions and sharing almost  
497 similar climatic conditions, but MODIS is found to be more successful in describing  
498 climatology over Solar Village than over Bahrain and this could be attributed to different

499 factors related to surface reflection, cloud coverage, and the large water body surrounding  
500 Bahrain. Thus in order to decrease data uncertainty, it is important to determine which sensor  
501 provides best retrieval over certain geographic location and AOD range.

502

### 503 **Acknowledgements**

504 The author would like to acknowledge the support provided by the Deanship of Scientific  
505 Research (DSR) at the King Fahd University of Petroleum and Minerals (KFUPM) for  
506 funding this work through project # IN161053. Portions of this work were performed at the  
507 Jet Propulsion Laboratory (JPL), California Institute of Technology, under a contract with  
508 the National Aeronautics and Space Administration. The author would like to thank Michael  
509 Garay (MJG) and Olga Kalashnikova (OVK) (JPL) for their suggestion of investigating  
510 satellites – AERONET matched data climatology, and discussion during the data analysis.  
511 The author would also like to thank Hesham El-Askary (Chapman University) for providing  
512 recommendation about AERONET data over North Africa and the Middle East as well as  
513 reviewing the English in the manuscript. We thank the MISR project for providing facilities,  
514 and supporting contributions of MJG and OVK. Finally, we thank the reviewers for  
515 suggestions, which improved the manuscript.

516

517

518 **Author Contributions:** Ashraf Farahat analysed the data, performed the statistical analysis  
519 and wrote the manuscript.

520

521 **Conflicts of Interest:** The authors declare no conflict of interest.

522

523

524

525

526

527

528

### 529 **References**

530 1. Abdi, V., Flamant, C., Cuesta, J., Oolman, L., Flamant, P., and Khaledifard, H. R.  
531 Dust transport over Iraq and northwest Iran associated with winter Shamal: A case  
532 study. *J. Geophys. Res.*, 117, D03201, 2013.

533

534 2. Ackerman, S., Strabala, K. I., Menzel, W. P., Frey, R. A., Moeller, C. C. and Gumley,  
535 L. E. (1998): Discriminating clear sky from clouds with MODIS. *J. Geophys. Res.*,  
536 103, 32 141–157, 1998.

- 537
- 538 3. Afnan, F. Heavy metal, trace element and petroleum hydrocarbon pollution in the  
539 Arabian Gulf: Review, *Journal of the Association of Arab Universities for Basic and*  
540 *Applied Sciences*, 17, 90-100, 2015.
- 541
- 542 4. Ansmann, A., Petzold, A., Kandler, K., Tegen, I., Wendisch, M., Müller, D.,  
543 Weinzierl, B., Müller, T., and Heintzenberg, J. Saharan Mineral Dust Experiments  
544 SAMUM-1 and SAMUM-2: what have we learned? *Tellus B*, 63, 403–429, 2011.
- 545
- 546 5. Basart, S., Pérez, C., Cuevas, E., Baldasano, J. M., and Gobbi., G. P. Aerosol  
547 characterization in Northern Africa, Northeastern Atlantic, Mediterranean Basin and  
548 Middle East from direct-sun AERONET observations. *Atmos. Chem. Phys.*, 9, 8265-  
549 8282, 2009.
- 550
- 551 6. Böer B., An introduction to the climate of the United Arab Emirates (review). *J*  
552 *Arid Environ*, 35:3–16, 1997.
- 553
- 554 7. Bou Karam, D., Flamant, C., Cuesta, J., Pelon, J., and Williams, E. Dust emission  
555 and transport associated with a Saharan depression: February 2007 case, *J.*  
556 *Geophys. Res.*, 115, D00H27, 2010.
- 557
- 558 8. Bre´on, F-M., Vermeulen, A., Descloitres, J. An evaluation of satellite aerosol  
559 products against sunphotometer measurements. *Remote Sensing Environ.*, 115,  
560 3102–11, 2011.
- 561
- 562 9. Bruegge, C., Chrien, N., Kahn, R., Martonchik, J., and Diner, D. MISR radiometric  
563 uncertainty analyses and their utilization within geophysical retrievals. *IEEE Trans.*  
564 *Geosci. Remote Sens.*, 36, 1186- 1198, 1998.
- 565
- 566
- 567 10. Chin, M., Diehl, T., Tan, Q., Prospero, J. M., Kahn, R. A., Remer, L. A., Yu, H.,  
568 Sayer, A. M., Bian, H., Geogdzhayev, I. V., Holben, B. N., Howell, S. G.,  
569 Huebert, B. J., Hsu, N. C., Kim, D., Kucsera, T. L., Levy, R. C.,  
570 Mishchenko, M. I., Pan, X., Quinn, P. K., Schuster, G. L., Streets, D. G.,  
571 Strode, S. A., Torres, O., and Zhao, X.-P. Multi-decadal aerosol variations from  
572 1980 to 2009: a perspective from observations and a global model, *Atmos. Chem.*  
573 *Phys.*, 14, 3657-3690, 2014.
- 574
- 575 11. Chu, D. A., Kaufman, Y. J., Remer, L. A., and Holben, B. N. Remote sensing of  
576 smoke from MODIS airborne simulator during the SCAR-B experiment. *J. Geophys.*  
577 *Res.*, 103, 31, 979– 987, 1998.
- 578
- 579 12. Derimian, Y., Karnieli, A., Kaufman, Y. J., Andreae, M. O., Andreae, T. W.,  
580 Dubovik, O., Maenhaut, W., Koren, I., and Holben, B. N. Dust and pollution  
581 aerosols over the Negev desert, Israel: Properties, transport, and radiative effect. *J.*  
582 *Geophys. Res.*, 111, D05205, 2006.

583  
584  
585  
586  
587  
588  
589  
590  
591  
592  
593  
594  
595  
596  
597  
598  
599  
600  
601  
602  
603  
604  
605  
606  
607  
608  
609  
610  
611  
612  
613  
614  
615  
616  
617  
618  
619  
620  
621  
622  
623  
624  
625  
626  
627  
628  
629  
630  
631  
632

13. Dubovik, O. and King, M. D. A flexible inversion algorithm for retrieval of aerosol optical properties from Sun and sky radiance measurements. *J. Geophys. Res.*, 105 206730–20696, 2000.
14. Dubovik, O., Holben, B. N., Eck, T. F., Smirnov, A., Kaufman, Y. J., King, M. D. Tanre, D., and Slutsker, I. Variability of absorption and optical properties of key aerosol types observed in worldwide locations. *J. Atmos. Sci.*, 59, 590–608, 2002.
15. Dubovik, O., Sinyuk, A., Lapyonok, T., Holben, B., Mischenko, M., Yang, P., Eck, T., Volten, H., Muñoz, O., Veihelmann, B., van der Zande, W. J., Leon, J.-F., Sorokin, M., and Slutsker, I. The application of spheroid models to account for aerosol particle non-sphericity in remote sensing of desert dust. *J. Geophys. Res.*, 111, D11208, 2006.
16. Eck, T., Holben, B. N., Reid, J. S., O'Neill, N. T., Schafer, J. S., Dubovik, O., Smirnov, A., Yamasoe, M. A., and Artaxo, P. High aerosol optical depth biomass burning events: A comparison of optical properties for different source regions, *Geophys. Res. Lett.*, 200b, 30, 2035, 2003b.
17. Eck, T., et al. Climatological aspects of the optical properties of fine/coarse mode aerosol mixtures. *J. Geophys. Res.*, 115, D19205, 2010.
18. Elagib, N., Addin Abdu A. Climate variability and aridity in Bahrain. *J. Arid Environ.*, 36:405–419, 1997.
19. El-Askary H., Farouk R., Ichoku C., and Kafatos M. Inter-continental transport of dust and pollution aerosols across Alexandria, Egypt, *Annales Geophysicae*, 27, 2869–2879, 2009.
20. Farahat, A., El-Askary, H., and Al-Shaibani, A. Study of Aerosols' Characteristics and Dynamics over the Kingdom of Saudi Arabia using a Multi Sensor Approach Combined with Ground Observations. *Advances in Meteorology*, Article ID 247531, 2015.
21. Farahat, A. Air Pollution in Arabian Peninsula (Saudi Arabia, United Arab Emirates, Kuwait, Qatar, Bahrain, and Oman): Causes, Effects and Aerosol Categorization. *Arab J of Geosci.*, 9, 196, 2016.
22. Farahat, A., El-Askary, H., and Dogan, A. U., 2016: Aerosols size distribution characteristics and role of precipitation during dust storm formation over Saudi Arabia. *Aerosol Air Qual. Res.*, 16, 2523-2534, 2016.
23. Farahat, A., El-Askary, H., Adetokunbo, P., Abu-Tharr, F. Analysis of aerosol absorption properties and transport over North Africa and the Middle East using AERONET data. *Annales Geophysicae.*, 34:11, 1031-1044, 2016.
24. He, Q., Li, C., Tang, X., Li, H., Geng, F., Wu, Y. Validation of MODIS derived aerosol optical depth over the Yangtze River Delta in China. *Remote Sensing Environ.*, 114, w21649–61, 2010.

- 633  
634 25. Higurashi, A., and Nakjima, T. Development of a two-channel aerosol retrieval  
635 algorithm on a global scale using NOAA AVHRR. *J. Atmos. Sci.*, 56, 924–941,  
636 1999.
- 637  
638 26. Holben, B., Eck, T., Slutsker, I., Tanre, D., Buis, J., Setzer, A. et al. AERONET—  
639 A federated instrument network and data archive for aerosol characterization.  
640 *Remote Sensing Environ.*, 66, 1–16, 1998.  
641
- 642 27. Holben, B., Smirnov, A., Eck, T., Slutsker, I., Abuhassan, N., Newcomb, W., et al.  
643 An emerging ground-based aerosol climatology—Aerosol optical depth from  
644 AERONET, *J. Geophys Res.*, 106, 12067–97, 2001.  
645
- 646 28. Hoell, A., Funk, C., and Barlow, M. The regional forcing of Northern Hemisphere  
647 drought during recent warm tropical west Pacific Ocean La Niña events. *Clim.*  
648 *Dyn.*, 42, 3289–3311, 2013.  
649  
650
- 651 29. Hsu, N., Gautam, R., Sayer, A., Bettenhausen, C., Li, C., Jeong, M., Tsay, S., and  
652 Holben, B. Global and regional trends of aerosol optical depth over land and ocean  
653 using SeaWiFS measurements from 1997 to 2012. *Atmos. Chem. Phys.*, 12, 8037–  
654 8053, 2012.  
655
- 656 30. Ichoku, C., Chu, D. A., Mattoo, S., Kaufman, Y. J., Remer, L. A., Tanre, D.,  
657 Slutsker, I., and Holben, B. N. A spatio-temporal approach for global validation  
658 and analysis of MODIS aerosol product, *Geophys. Res. Lett.*, 29, 12, 8006, 2002.  
659
- 660 31. Ginoux, P., Chin, M., Tegen, I., Prospero, J., Holben, B., Dubovik, O., and Lin, S.-  
661 J. Sources and global distributions of dust aerosols simulated with the GOCART  
662 model, *J. Geophys. Res.*, 106, 20255 – 20273, 2001.  
663
- 664 32. Kahn, R. A., Gaitley, B. J., Martonchik, J. V., Diner, D. J., Crean, K. A. and Holben,  
665 B. Multiangle ImagingSpectroradiometer (MISR) global aerosol optical depth  
666 validation based on 2 years of coincident Aerosol Robotic Network (AERONET)  
667 observations, *J. Geophys. Res.*, 110, 2005.  
668
- 669 33. Kahn, R., Garay, M., Nelson, D., Yau, K., Bull, M., Gaitley, B. et al. Satellite-  
670 derived aerosol optical depth over dark water from MISR and MODIS:  
671 Comparisons with AERONET and implications for climatological studies. *J.*  
672 *Geophys. Res.*, 112, D18205, 2007.  
673
- 674 34. Kahn, R., Nelson, D., Garay, M., Levy, R., Bull, M., Diner, D., et al. MISR aerosol  
675 product attributes, and statistical comparisons with MODIS. *IEEE Trans Geosci*  
676 *Remote Sensing*, 47, 4095–114, 2009.  
677
- 678 35. Kim, D., Chin, M., Bian, H., Tan, Q., Brown, M. E., Zheng, T., You, R., Diehl, T.,  
679 Ginoux, P., and Kucsera, T. The effect of the dynamic surface bareness on dust  
680 source function, emission, and distribution, *J. Geophys. Res.*, 118, 1–16, 2013.  
681



- 682 36. Kaufman, Y., Tanre, D., Remer, L., Vermote, E., Chu, A., and Holben, B.  
683 Operational remote sensing of tropospheric aerosol over land from EOS moderate  
684 resolution imaging spectroradiometer. *J. Geophys. Res.-Atmos.*, 102, D14, 17051–  
685 17067, 1997.  
686
- 687 37. Kokhanovsky, A., Breon, F., Cacciari, A., Carboni, E., Diner, D., Di Nicolantonio,  
688 W. et al. Aerosol remote sensing over land: a comparison of satellite retrievals using  
689 different algorithms and instruments. *Atmos Res.*, 85, 372–94, 2007.  
690
- 691 38. Liu, L., Mishchenko, M. Toward unified satellite climatology of aerosol properties:  
692 direct comparisons of advanced level 2 aerosol products. *JQSRT.*, 109, 2376–85,  
693 2008.  
694
- 695 39. Marey, H., Gille, J., El-Askary, H., Shalaby, E. , and El- Raey, M. Study of the  
696 formation of the “black cloud and its dynamics over Cairo, Egypt, using MODIS  
697 and MISR sensors. *J. Geophys. Res.*, 115, D21206, 2010.  
698
- 699 40. Martonchik, J., Diner, D., Crean, K., and Bull. M. Regional aerosol retrieval results  
700 from MISR. *IEEE Trans. Geosci. Remote Sens.*, 40, 1,520–1,531, 2002.  
701
- 702 41. Mishchenko, M., I. Geogdzhayev, L. Liu, A. Lacis, B. Cairns, L. Travis. Toward  
703 unified satellite climatology of aerosol properties: what do fully compatible  
704 MODIS and MISR aerosol pixels tell us? *J Quant Spectrosc Radiat Transfer.* 110,  
705 402–8, 2009.  
706
- 707 42. Mishchenko, M., Liu, L., Geogdzhayev, I., Travis, L., Cairns, B., Lacis, A. Toward  
708 unified satellite climatology of aerosol properties: 3. MODIS versus MISR versus  
709 AERONET. *J Quant Spectrosc Radiat Transfer.*, 111, 540–52, 2010.  
710
- 711 43. Remer, L., Kaufman, Y., Tanre´, D., Mattoo, S., Chu, D., Martins, J., et al. The MODIS  
712 aerosol algorithm, products, and validation. *J Atmos Sci.*, 62, 947–73, 2005.  
713
- 714 44. Sadiq, M. and McCain, J. *The Gulf War Aftermath: An Environmental Tragedy.*,  
715 1<sup>st</sup> ed., Springer, 1993.  
716
- 717 45. Sayer, A., Hsu, N., Eck, T., Smirnov, A., and Holben, B. AERONET-based models  
718 of smoke-dominated aerosol near source regions and transported over oceans, and  
719 implications for satellite retrievals of aerosol optical depth. *Atmos. Chem. Phys.*,  
720 14, 11493-11523, 2014.  
721
- 722 46. Schepanski, K., Mallet, M., Heinold, B., and Ulrich, M.: North African dust  
723 transport toward the western Mediterranean basin: atmospheric controls on dust  
724 source activation and transport pathways during June–July 2013, *Atmos. Chem.*  
725 *Phys.*, 16, 14147-14168, 2016.  
726
- 727 47. Sioris, C. E., McLinden, C. A., Shephard, M. W., Fioletov, V. E., and Abboud, I.:  
728 Assessment of the aerosol optical depths measured by satellite-based passive  
729 remote sensors in the Alberta oil sands region, *Atmos. Chem. Phys.*, 1931-1943,  
730 2017.  
731

732 48. Smirnov, A., Holben, B., Eck, T., Dubovik, O., and Slutsker, I. Cloud-screening  
733 and quality control algorithms for the AERONET data-base, *Remote Sens.*  
734 *Environ.*, 73, 337 – 349, 2000.  
735

736 49. Solomos, S., Ansmann, A., Mamouri, R.-E., Biniotoglou, I., Patlakas, P., Marinou,  
737 E., and Amiridis, V. Remote sensing and modelling analysis of the extreme dust  
738 storm hitting the Middle East and eastern Mediterranean in September 2015,  
739 *Atmos. Chem. Phys.*, 17, 4063-4079, 2017.

740

741 50. Todd M., R. Washington, Vanderlei, M., Dubovik, O., Lizcano, G., M’Bainayel,  
742 S., Engelstaedter, S. Mineral dust emission from the Bodélé Depression, northern  
743 Chad, during BoDEx 2005. *J. Geophys. Res.*, 112. D06207, 2007.  
744

745 51. Von Hoyningen-Huene, W., Posse, P. Nonsphericity of aerosol particles and their  
746 contribution to radiative forcing. *JQSRT*, 57, 651–68, 1997.  
747  
748

749 52. Yu, Y., Notaro, M., Liu, Z., Kalashnikova, O., Alkolibi, F., Fadda, E., and Bakhrjy,  
750 F. Assessing temporal and spatial variations in atmospheric dust over Saudi Arabia  
751 through satellite, radiometric, and station data, *J. Geophys. Res. Atmos.*, 118, 13,  
752 253–13, 264, 2013.  
753

754 53. Yu, Y., Notaro, M., Liu, Z., Wang, F., Alkolibi, F., Fadda, E. and Bakhrjy,  
755 F. Climatic controls on the interannual to decadal variability in Saudi Arabian dust  
756 activity: Toward the development of a seasonal dust prediction model. *J. Geophys.*  
757 *Res. Atmos.*, 120, 1739–1758, 2015.  
758

759 54. Zhao, G. and Girolamo, L. A cloud fraction versus view angle technique for  
760 automatic in-scene evaluation of the MISR cloud mask. *J. Appl. Meteorol.*, 43, 6,  
761 860–869, 2004.

762

763

764

765

766

767

768

769

770

771

772

773 **Tables' caption**

774 Table 1. Geographic location of the AERONET sites used in this study

775 Table 2. Statistics for dust sites, R: correlation coefficient, RMSE: Root Mean Square  
776 deviation; G-fraction: good fraction; N: number of observations

777 Table 3. Statistics for biomass and mixed sites, parameters as in Table 3. Caption.

778 Table 4. MISR coverage for six days of major dust activity over the Arabian Peninsula  
779 during March 2009.

780

781

782

783

784

785

786

787

788

789

790

791

792

793

794

795

796

797

798 **Figures caption**

799 Figure 1. Location of the AERONET stations over North Africa and the Middle East. The  
800 numbers on the map indicates the site location as 1: Saada, 2: Tamanrasset\_INM, 3: Cairo,  
801 4: Sede Boker, 5: Solar Village, 6: Mezaira, 7: Bahrain.

802 Figure 2. Scatter plot of MISR AOD versus AERONET AOD based on seasons and  
803 aerosols categorization.

804 Figure 3. Scatter plot of MODIS AOD versus AERONET AOD based on seasons and  
805 aerosols categorization.

806 Figure 4. Time series of monthly mean AOD derived from MODIS/Aqua, MODIS/Terra,  
807 MISR and AERONET over a) dust b) biomass and c) mixed dominated aerosol regions.

808 Figure 5. Long range AOD difference for MODIS/Terra and MODIS/Aqua over the dust,  
809 biomass and mixed sites.

810 Figure 6. Histogram of the MISR, MODIS and Solar Village AERONET measurements a)  
811 MISR b) MODIS data retrievals.

812 Figure 7. Histogram of the MISR, MODIS and Mezaria AERONET measurements a)  
813 MISR b) MODIS data retrievals.

814 Figure 8. Histogram of the MISR, MODIS and Bahrain AERONET measurements a) MISR  
815 b) MODIS data retrievals.

816 Figure 9. Histogram of the MISR, MODIS and SAADA AERONET measurements a)  
817 MISR b) MODIS data retrievals.

818 Figure 10. Histogram of the MISR, MODIS and Taman AERONET measurements a)  
819 MISR b) MODIS data retrievals.

820 Figure 11. Histogram of the MISR, MODIS and SEDEE Boker AERONET measurements  
821 a) MISR b) MODIS data retrievals.

822 Figure 12. Histogram of the MISR, MODIS and Cairo AERONET measurements a) MISR  
823 b) MODIS data retrievals.

824

825

826

827

828

829

Table 1.

<b>Location name</b>	<b>Lon./Lat.</b>	<b>Measurement period</b>
<b>Solar Village</b>	24.907° N/46.397° E	2000-2015
<b>Mezaria</b>	23.105° N/53.755° E	2004-2015
<b>Bahrain</b>	26.208° N/50.609° E	2000-2006
<b>Saada</b>	31.626° N/8.156° W	2003-2015
<b>Taman</b>	22.790° N/5.530° E	2000-2015
<b>Cairo</b>	30.081° N/31.290° E	2005 -2007
<b>Sede Boker</b>	30.855° N/34.782 ° E	2000-2015

830

831

832

833

834

835

836

837

838

839

<b>AERONET</b>	<b>Sensor</b>	<b>Season</b>	<b>Mean Value</b>	<b>N</b>	<b>R</b>	<b>Gfraction (%)</b>	
<b>Site</b>			<b>AERONET</b>	<b>Satellite</b>			
<b>Solar Village</b>	<b>MISR</b>	<b>DJF</b>	0.18±0.15	0.23±0.13	24	0.94	79.1
		<b>MAM</b>	0.45±0.21	0.47±0.20	43	0.94	86.0
		<b>JJA</b>	0.39±0.16	0.42±0.16	57	0.90	82.4
		<b>SON</b>	0.25±0.14	0.29±0.12	50	0.99	82.0
	<b>MODIS</b> <b>Terra</b>	<b>DJF</b>	0.27±0.19	0.33±0.17	1500	0.48	51.80
		<b>MAM</b>	0.36±0.24	0.26±0.17	389	0.68	90.23
		<b>JJA</b>	0.34±0.17	0.42±0.19	429	0.41	54.31
		<b>SON</b>	0.22±0.10	0.36±0.12	471	0.51	28.87
<b>Mezaria</b>	<b>MISR</b>	<b>DJF</b>	0.17±0.09	0.23±0.07	53	0.89	50.9
		<b>MAM</b>	0.34±0.18	0.37±0.18	41	0.90	78.0
		<b>JJA</b>	0.49±0.20	0.47±0.21	51	0.85	92.1
		<b>SON</b>	0.26±0.09	0.30±0.12	53	0.87	88.2
	<b>MODIS</b> <b>Terra</b>	<b>DJF</b>	0.32±0.15	0.35±0.19	198	0.86	74.74
		<b>MAM</b>	0.44±0.33	0.45±0.27	115	0.92	78.07
		<b>JJA</b>	0.39±0.14	0.43±0.20	89	0.81	71.91
		<b>SON</b>	0.28±0.13	0.30±0.16	97	0.87	77.31
<b>Bahrain</b>	<b>MISR</b>	<b>DJF</b>	0.19±0.10	0.30±0.10	9	0.73	33.3
		<b>MAM</b>	0.47±0.20	0.67±0.05	7	0.89	28.5
		<b>JJA</b>	0.45±0.21	0.74±0.21	21	0.69	23.8
		<b>SON</b>	0.32±0.13	0.45±0.16	22	0.98	45.4
	<b>MODIS</b> <b>Terra</b>	<b>DJF</b>	0.42±0.29	0.20±0.19	121	0.41	93.38
		<b>MAM</b>	0.50±0.28	0.13±0.15	25	0.26	96.00
		<b>JJA</b>	0.55±0.26	0.31±0.27	42	0.50	88.09
		<b>SON</b>	0.35±0.14	0.21±0.12	29	0.32	93.10

Table 3.

<b>AERONET</b>	<b>Method</b>	<b>Season</b>	<b>Mean Value</b>		<b>N</b>	<b>R</b>	<b>Gfraction</b>	
<b>Site</b>							<b>(%)</b>	
			AERONET	Satellite				
<b>SAADA</b>	<b>MISR</b>	<b>DJF</b>	0.07±0.02	0.07±0.02	43	0.93	100.0	
		<b>MAM</b>	0.17±0.10	0.17±0.09	47	0.89	93.6	
		<b>JJA</b>	0.30±0.14	0.31±0.14	53	0.93	93.1	
		<b>SON</b>	0.14±0.07	0.13±0.06	51	0.94	96.0	
	<b>MODIS</b>	<b>DJF</b>	0.23±0.16	0.32±0.21	550	0.57	57.8	
		<b>MAM</b>	0.24±0.18	0.39±0.23	90	0.43	44.4	
		<b>JJA</b>	0.30±0.17	0.45±0.18	201	0.40	45.2	
		<b>SON</b>	0.19±0.13	0.22±0.14	162	0.71	72.3	
	<b>Taman</b>	<b>MISR</b>	<b>DJF</b>	0.07±0.10	0.09±0.06	69	0.92	85.5
			<b>MAM</b>	0.22±0.18	0.25±0.22	86	0.97	81.3
			<b>JJA</b>	0.42±0.31	0.45±0.28	57	0.85	78.9
			<b>SON</b>	0.14±0.11	0.15±0.10	72	0.94	95.8
<b>MODIS</b>		<b>DJF</b>	0.19±0.22	0.18±0.16	319	0.67	81.8	
		<b>MAM</b>	0.24±0.19	0.22±0.17	67	0.55	83.5	
		<b>JJA</b>	0.37±0.32	0.29±0.20	69	0.69	84.0	
		<b>SON</b>	0.14±0.14	0.13±0.10	117	0.54	84.6	
<b>Cairo</b>		<b>MISR</b>	<b>DJF</b>	0.33±0.17	0.17±0.09	15	0.94	100.0
			<b>MAM</b>	0.35±0.13	0.33±0.15	39	0.99	82.0
			<b>JJA</b>	0.35±0.09	0.27±0.08	61	0.99	96.7
			<b>SON</b>	0.37±0.14	0.28±0.13	23	0.97	78.2
	<b>MODIS</b>	<b>DJF</b>	0.33±0.16	0.20±0.11	158	0.30	95.5	
		<b>MAM</b>	0.32±0.16	0.12±0.08	39	0.25	100.0	
		<b>JJA</b>	0.35±0.14	0.28±0.07	58	0.17	94.8	
		<b>SON</b>	0.38±0.19	0.20±0.09	29	0.07	93.8	

	<b>DJF</b>	0.11±0.06	0.13±0.05	10	0.87	90.0
	<b>MAM</b>	0.21±0.13	0.24±0.13	76	0.68	75.0
<b>MISR</b>	<b>JJA</b>	0.16±0.08	0.21±0.08	142	0.85	66.9
	<b>SON</b>	0.162±0.07	0.20±0.06	54	0.89	79.6
<b>SEDEE_BOKER</b>	<b>DJF</b>	0.16±0.12	0.23±0.14	1312	0.36	53.5
	<b>MAM</b>	0.21±0.18	0.24±0.19	338	0.34	65.6
<b>MODIS</b>	<b>JJA</b>	0.16±0.09	0.33±0.13	392	0.27	17.3
<b>Terra</b>	<b>SON</b>	0.16±0.09	0.23±0.12	477	0.46	58.4

845

846

847

848

849

850

851

852

853

854

855

856

857

858

859

860

861

862

863



864

Table 4.

	AERONET		MISR		MODIS	
	N	AOD	N	AOD	N	AOD
		% > 0.4		% > 0.4		% > 0.4
<b>Solar</b>	3893	27.17	684	32.8	2789	30.1
<b>Village</b>						
<b>Mezaria</b>	2245	28.01	547	45.7	498	40.7
<b>Bahrain</b>	1116	31.36	676	35.8	217	18.4
<b>SAADA</b>	2974	10.32	667	11.5	1004	34.6
<b>Taman</b>	798	15.78	845	22.6	572	9.4
<b>Cairo</b>	2222	38.79	620	17.7	284	4.2
<b>SEDEE</b>	5722	4.28	675	9.0	2519	12.8

865

866

867

868

869

870

871

872

873

874

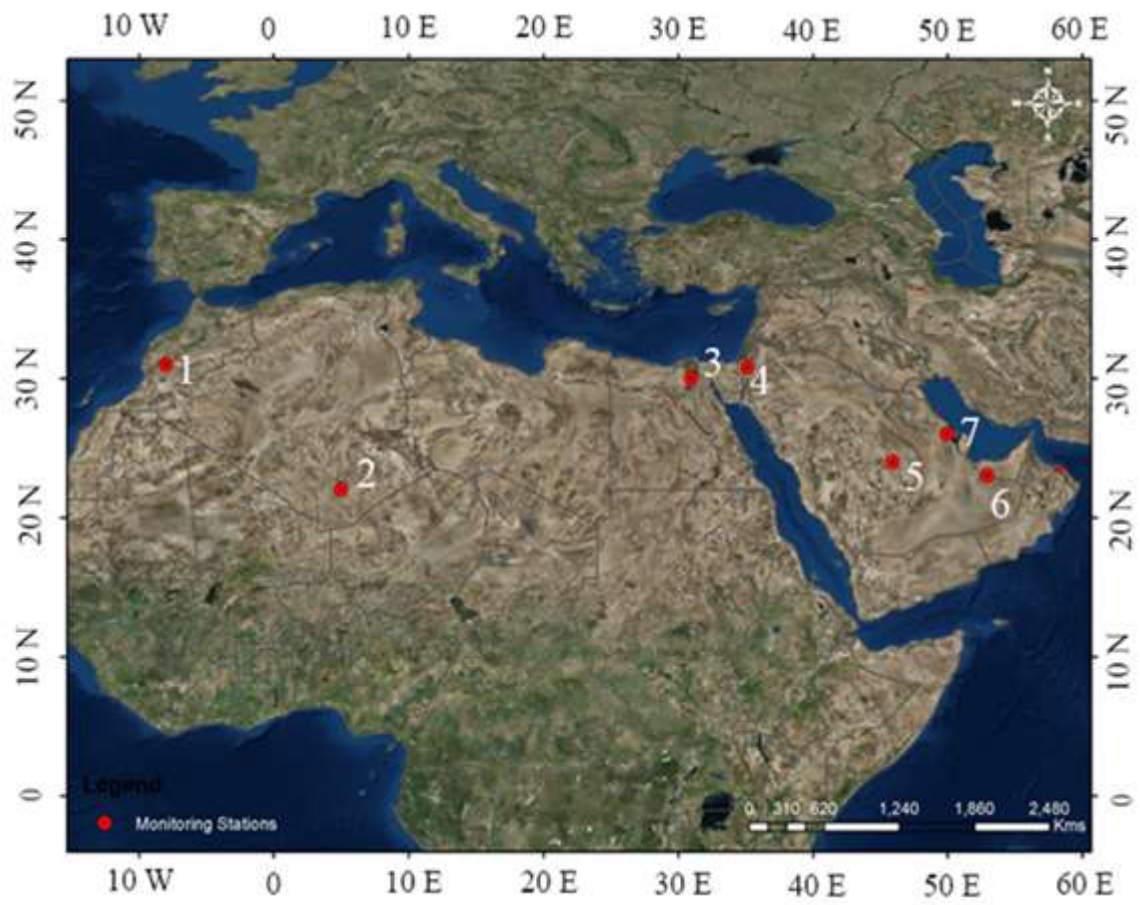
875

876

877

878

879



880

881

882 Figure 1.

883

884

885

886

887

888

889

890

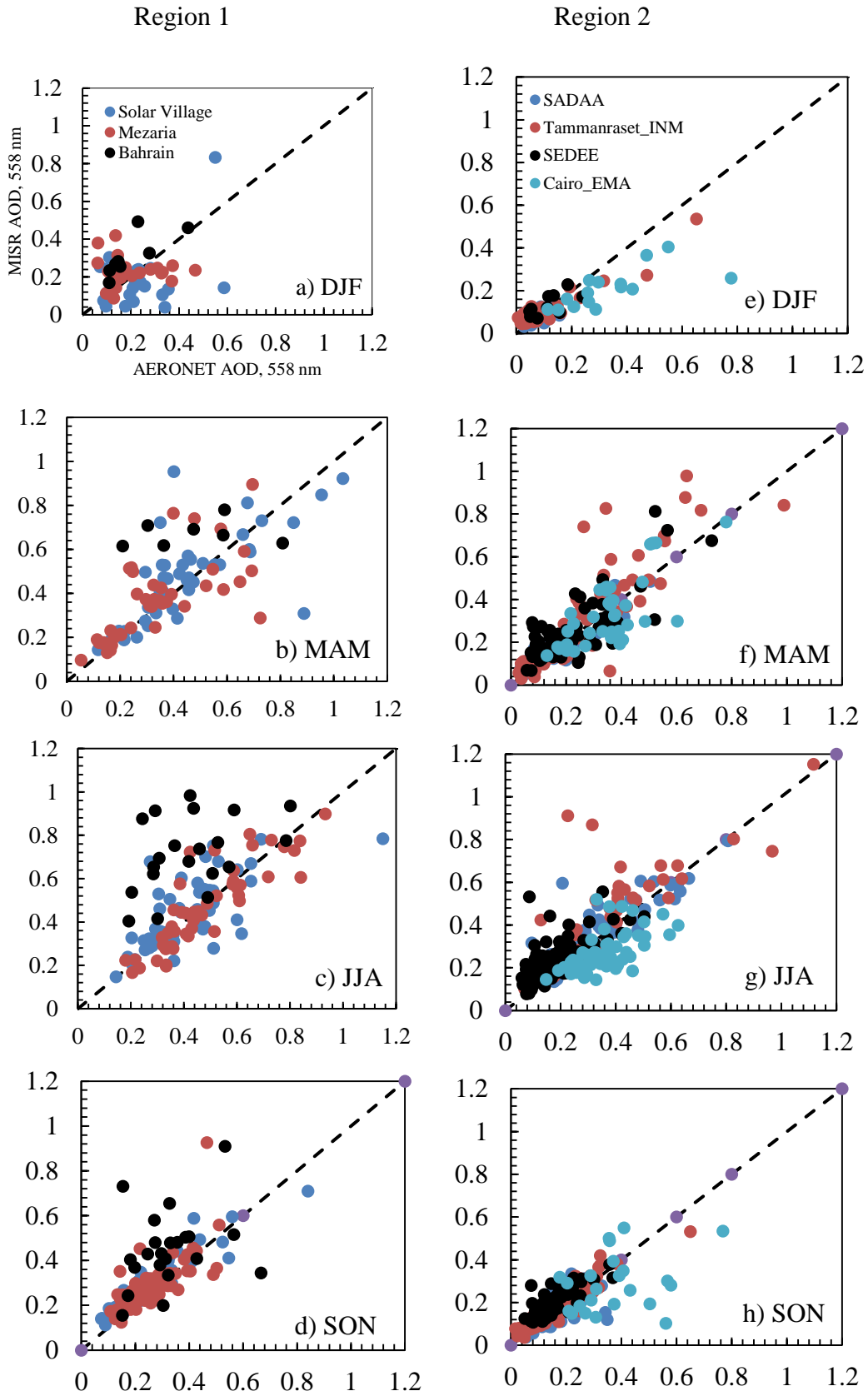


Figure 2

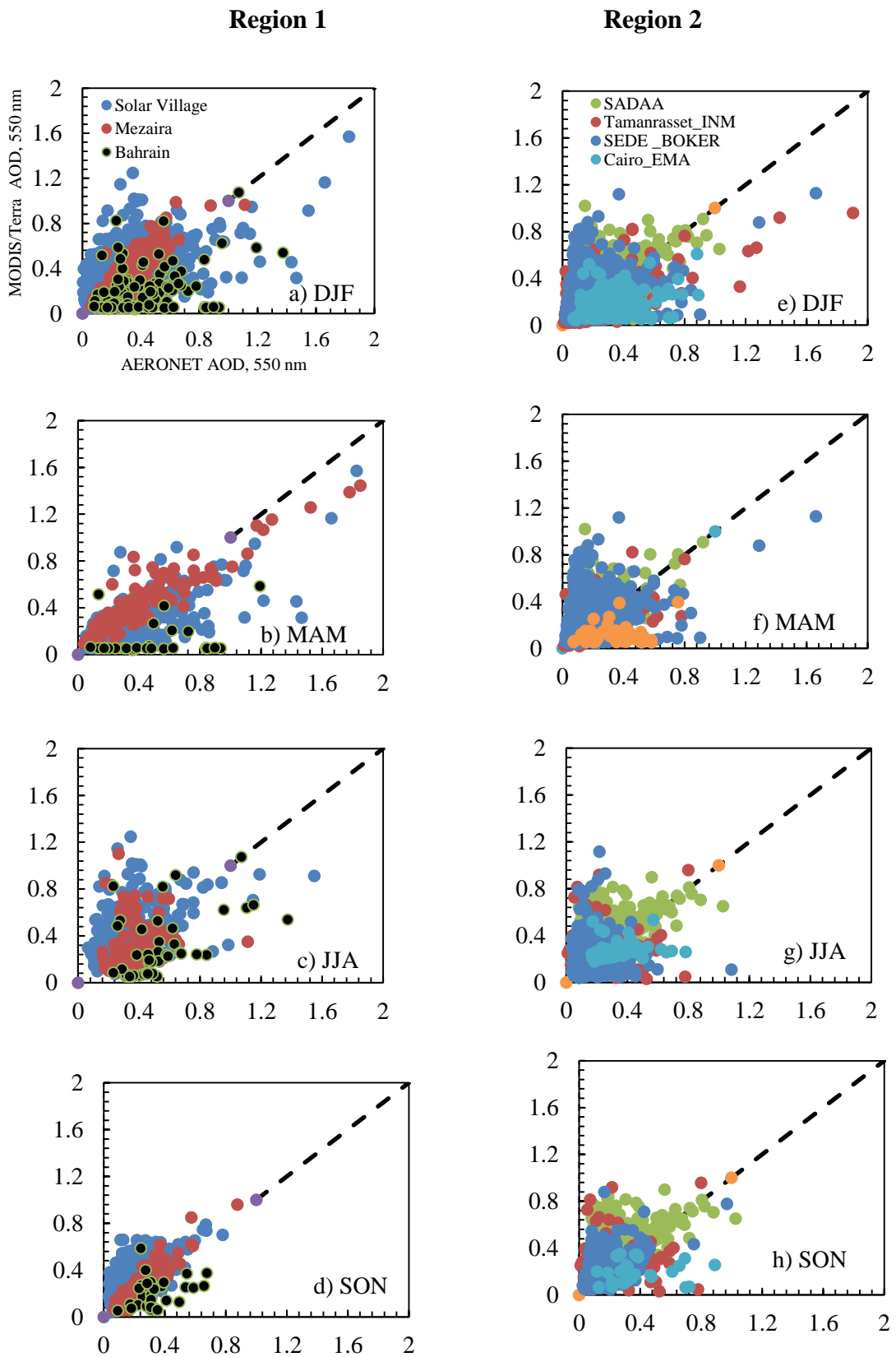
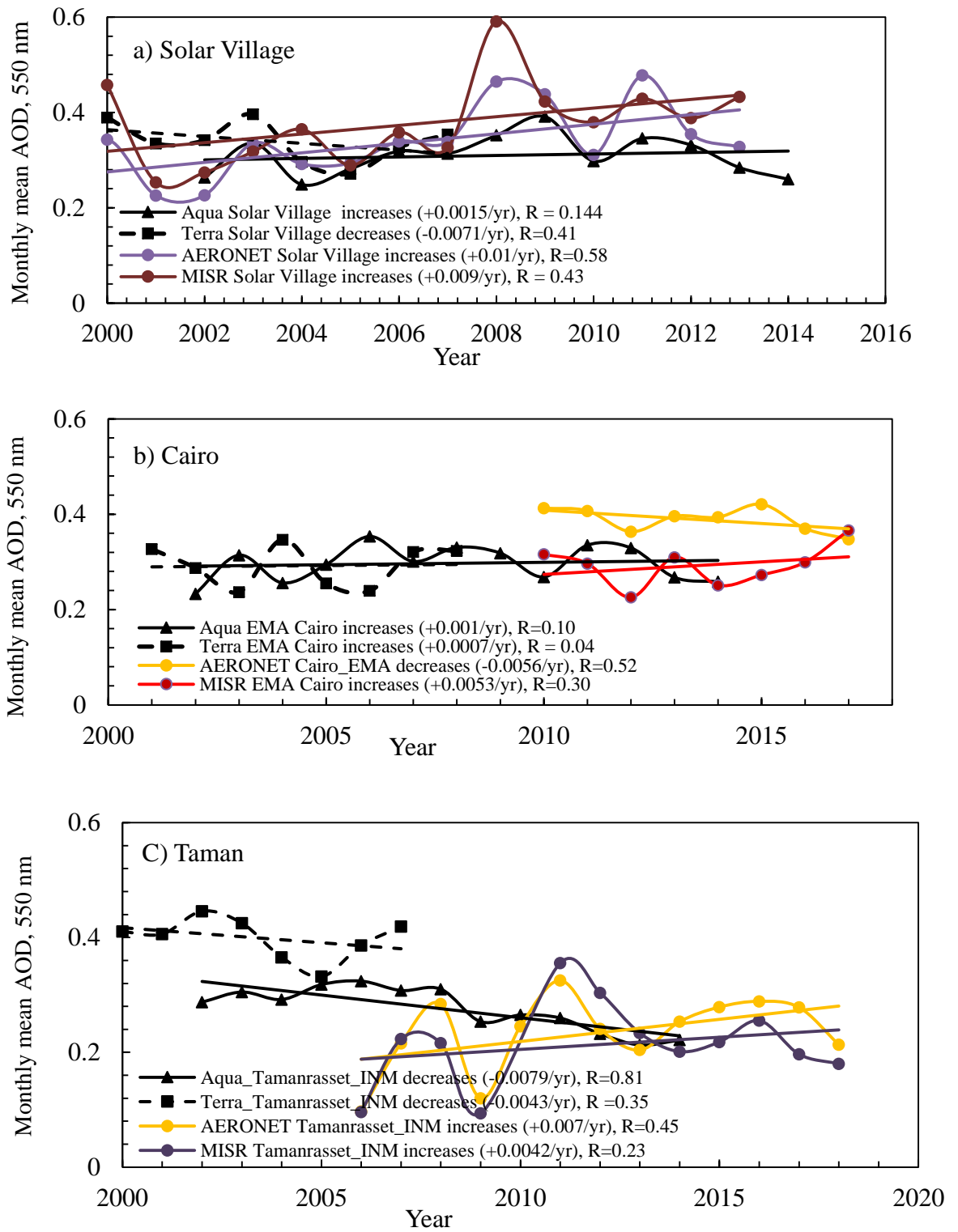


Figure 3.

898

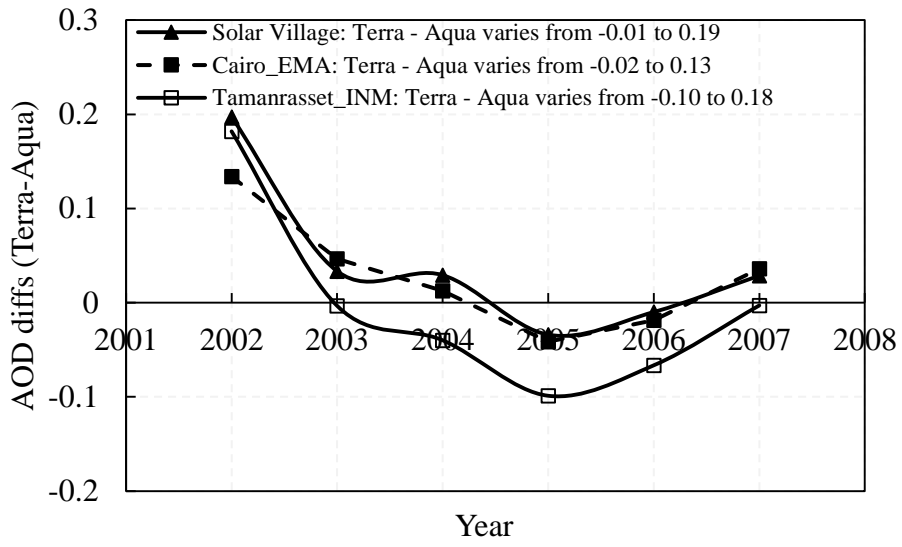
899

900



901 Figure 4.

902



911

912 Figure 5.

913

914

915

916

917

918

919

920

921

922

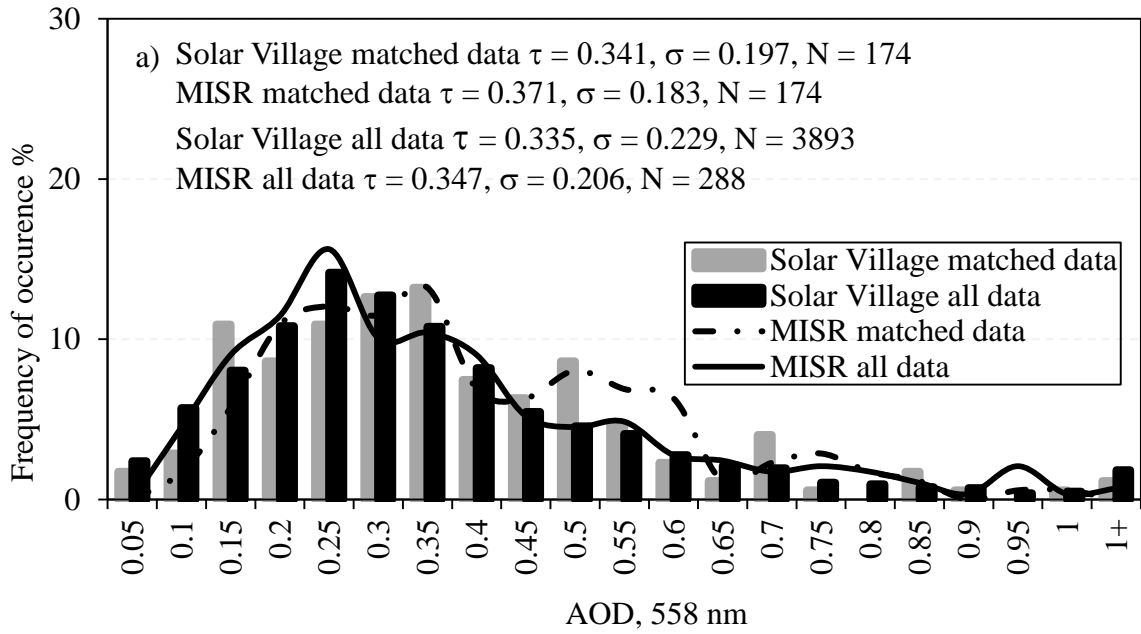
923

924

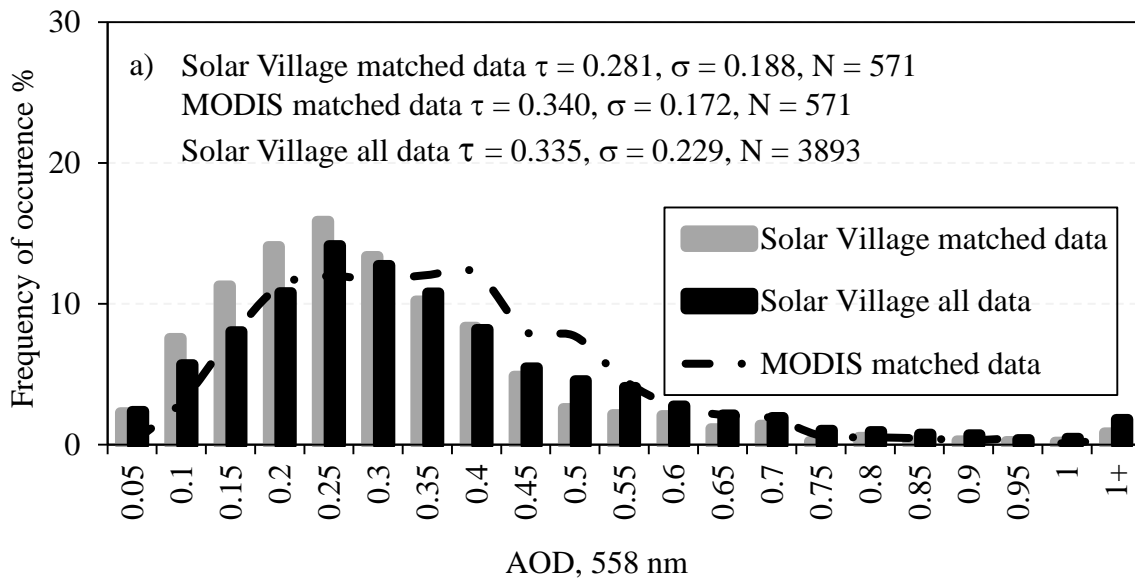
925

926

927



928



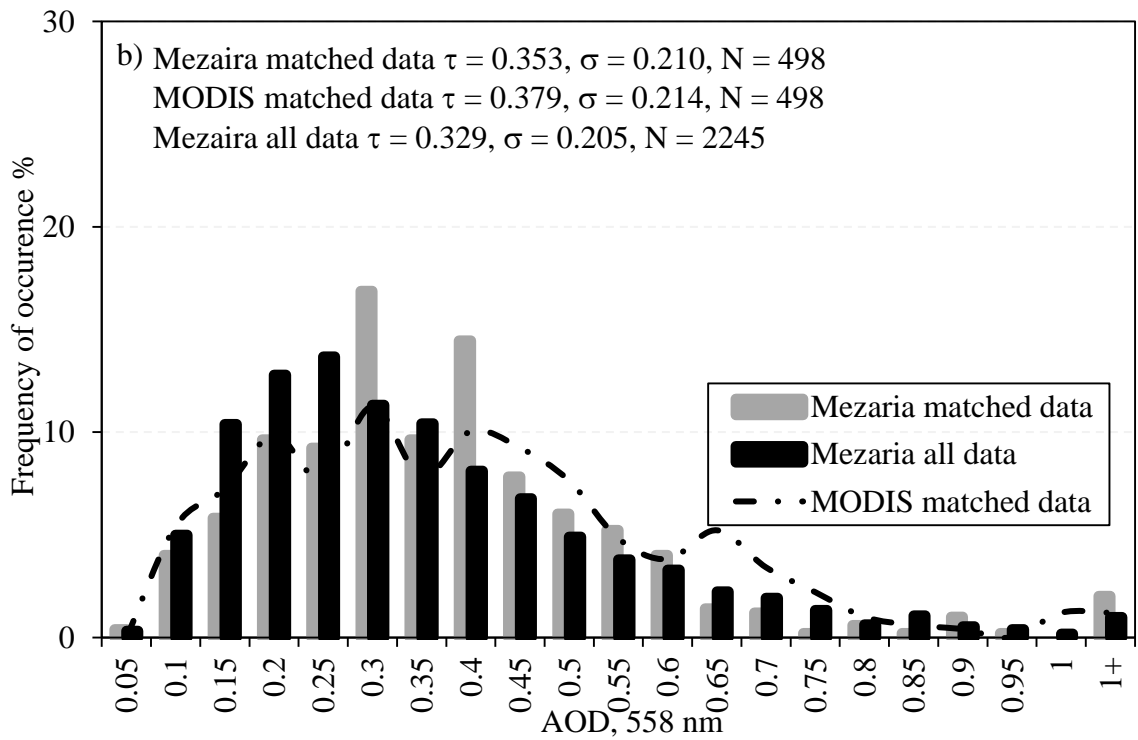
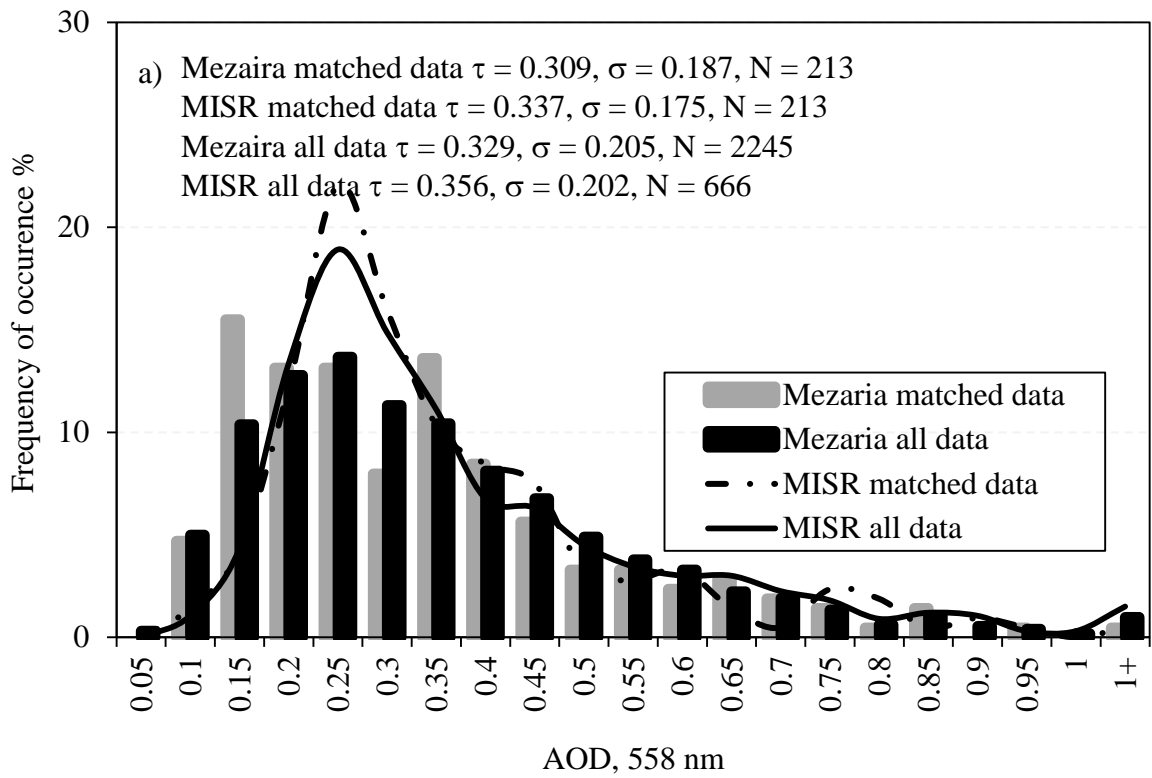
929

930 Figure 6.

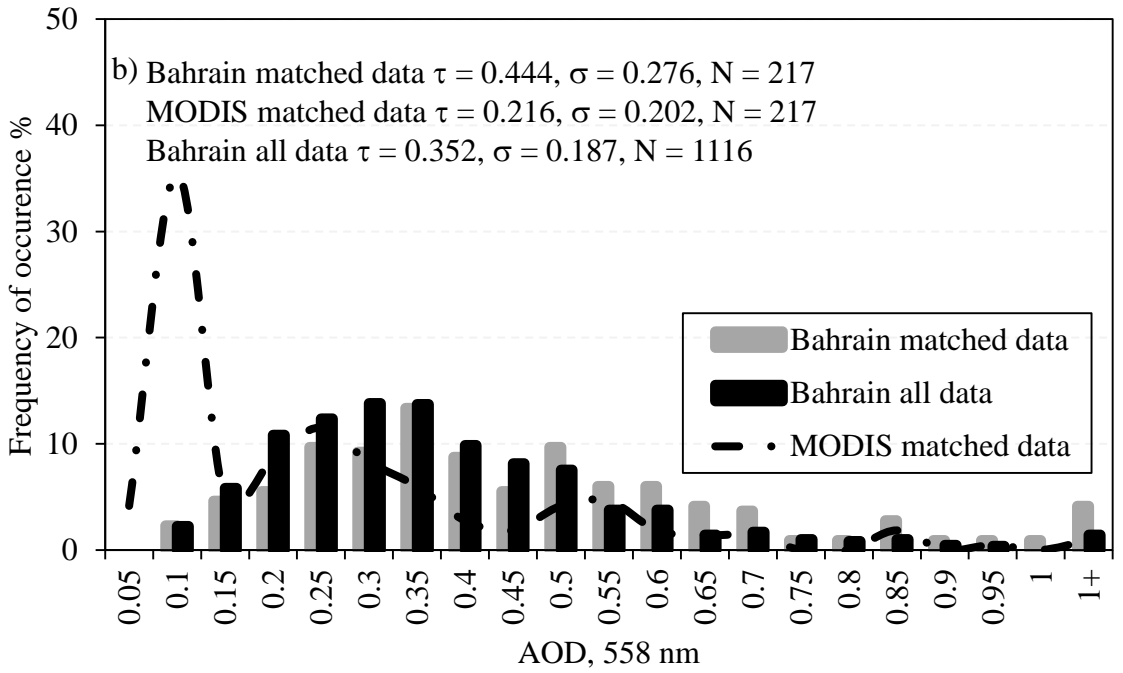
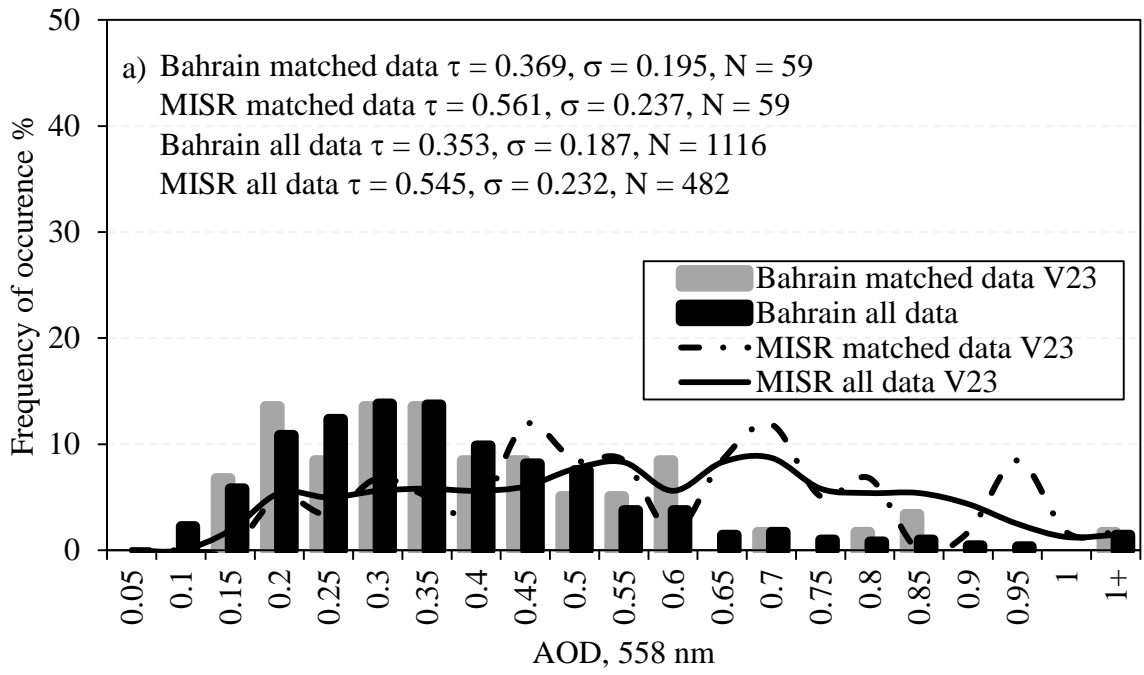
931

932

933





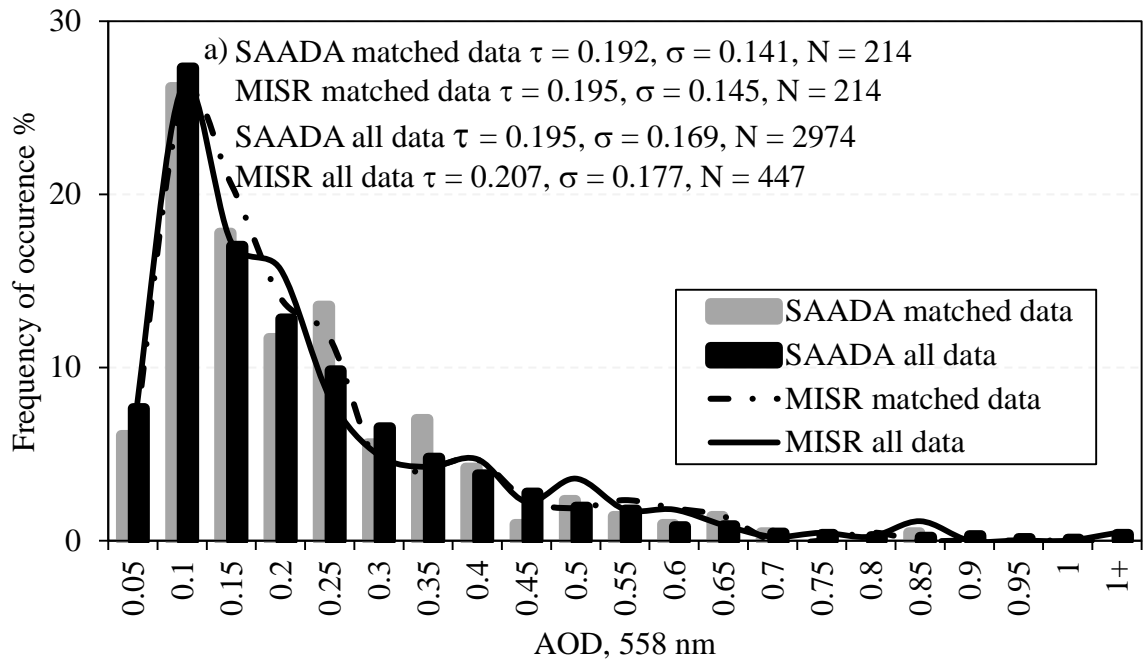


935

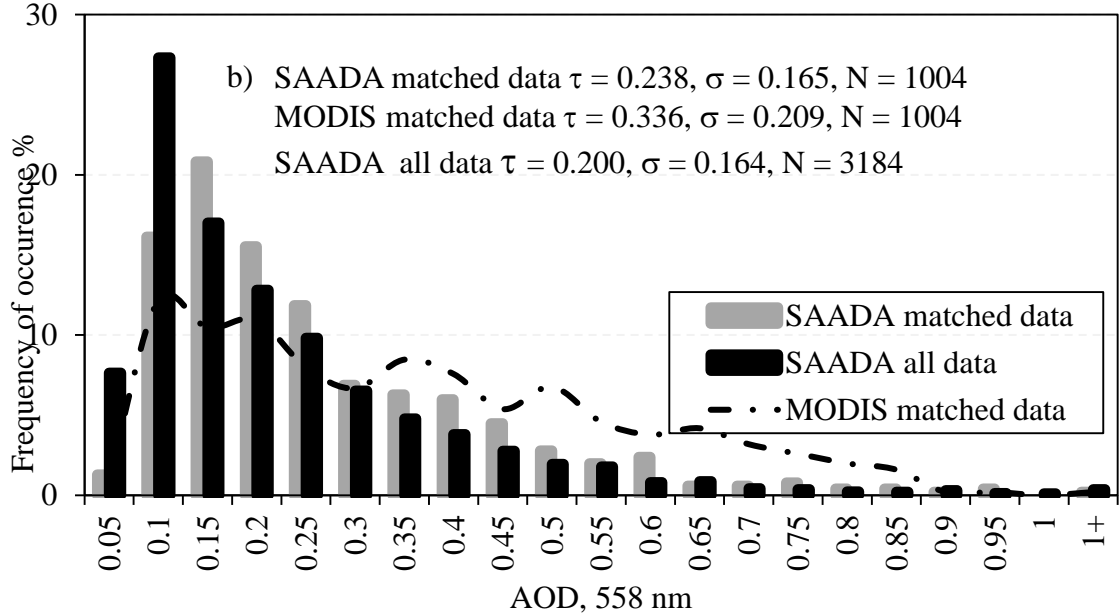
936

937 Figure 8.

938



939



940

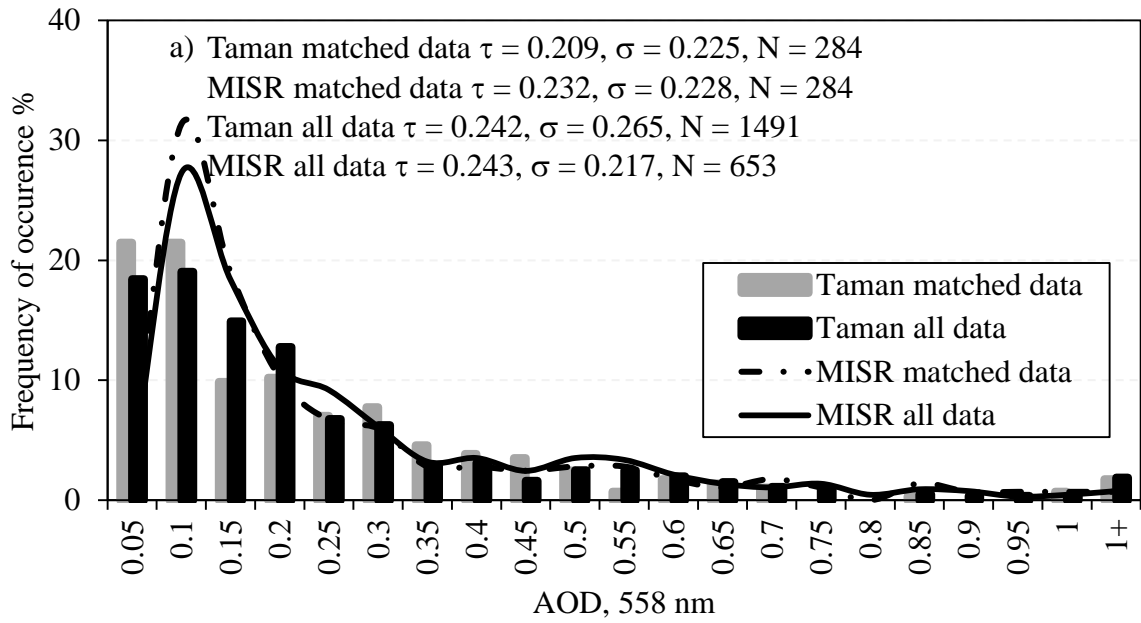
941 Figure 9.

942

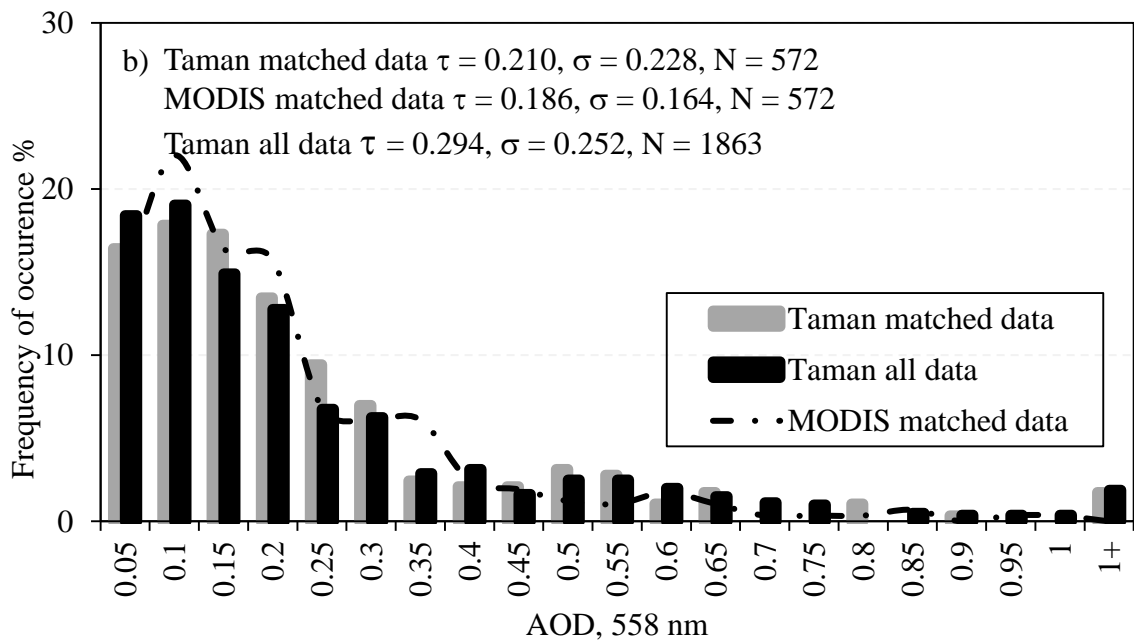
943

944

945



946



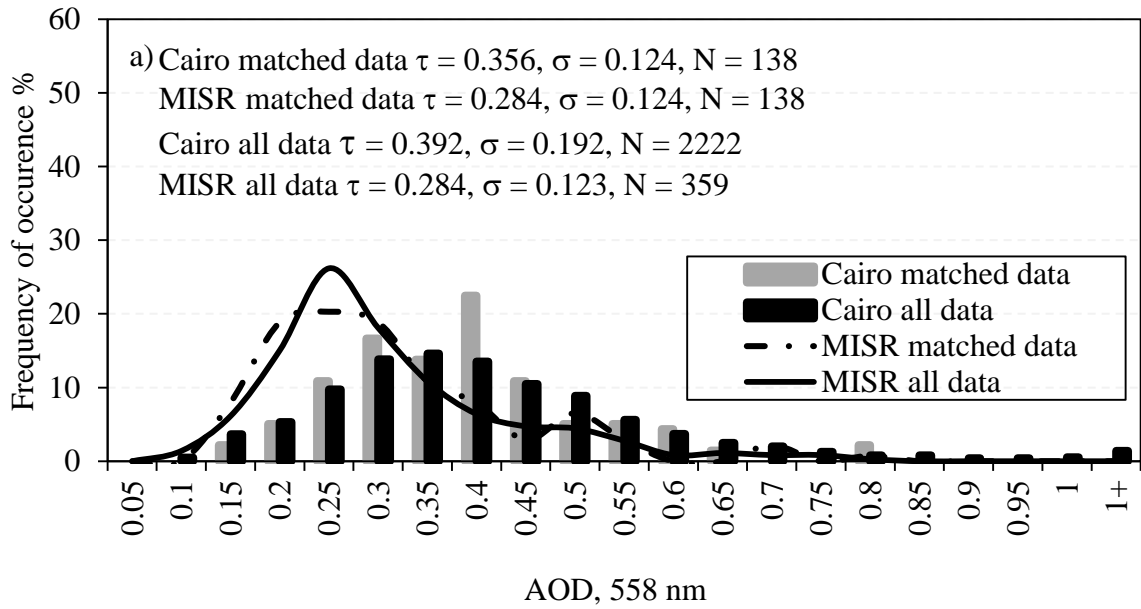
947

948 Figure 10.

949

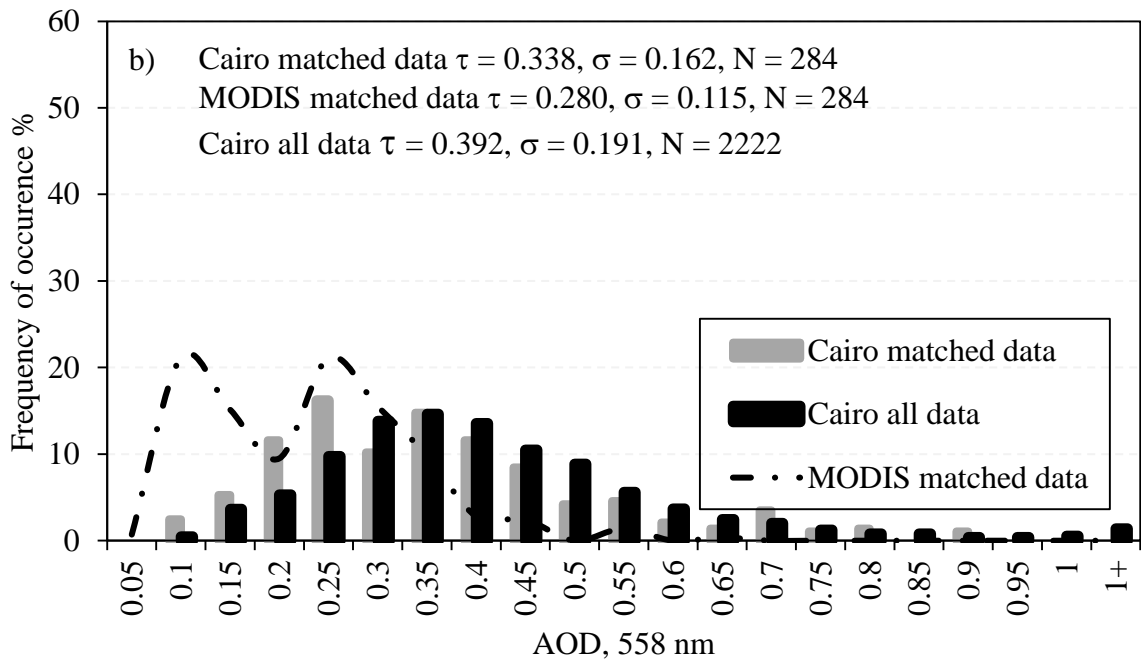
950

951



952

953

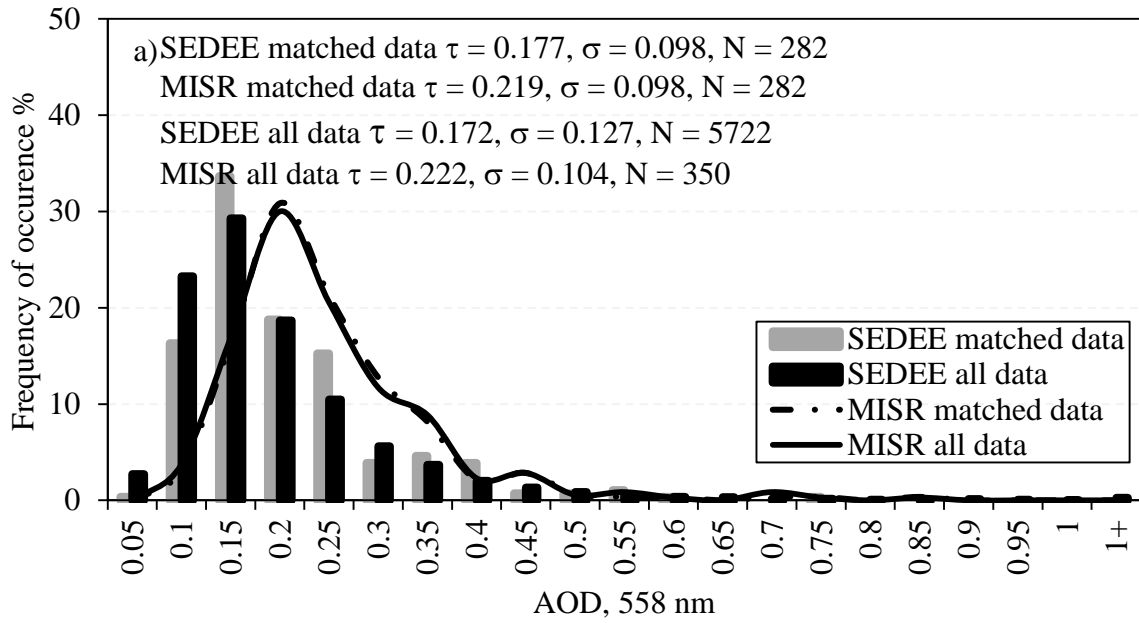


954 Figure 11.

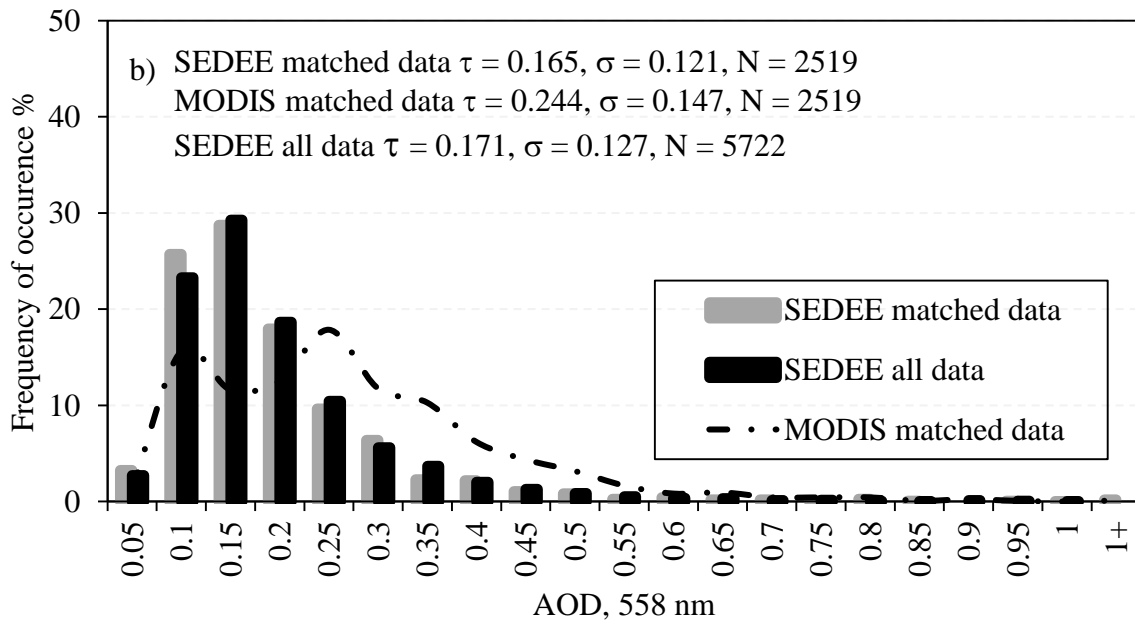
955

956

957



958



959

960 Figure 12.